Journal
of the
Optical Society of America
and
Review of Scientific Instruments

Vol. 17 JULY, 1928 Number 1

INVESTIGATION OF A LENS BY GRAPHICAL METHODS

By James P. C. Southall

1. *Introduction and Statement of the Problem to be Considered.*—A convenient graphical method of constructing the paths of typical rays through an optical system and of plotting the cardinal and "strategic" points affords an insight into the *modus operandi* of the instrument and its special peculiarities and advantages which can hardly ever be gained by the routine process of trigonometric calculation. Even in the preliminary design of such an instrument, an accurate geometrical drawing will often serve to show the nature of the modifications that are desirable in order to make the apparatus achieve more fully the purpose for which it is intended, although in the last analysis the test of exact trigonometric computation must be rigorously applied. In the first part of his presidential address on "Some uncultivated optical fields,"* Mr. Thomas Smith treats a number of problems of this kind in a way that is not only highly ingenious and original but, as it seems to me, likely to prove of great practical usefulness in optical engineering. Thus, for example, in the case of the so-called secondary imagery of a single spherical refracting surface, in which only the sagittal pencils of rays are concerned, he shows that for a given point of incidence the conjugate surfaces over which the value of the magnification-ratio is uniform are spheres with their centres all lying on the incidence-normal; whereas conjugate planes, such as the principal planes, nodal planes, etc., that are so distinguished in the theory of collinear imagery, are merely the planes tangent to the conjugate spheres at the points where they

*Delivered before the Optical Society of London, Feb. 10, 1927; published in the Trans. of the Optical Society, *28*, pp. 225–284; 1926–7.

intersect the incidence-normal. As this new point of view (to which Mr. Smith has frequently alluded in his previous writings on geometrical optics) seemed to me worthy of further investigation, I pursued the study of it in a recent paper contributed to this journal,* to which I shall have occasion to refer again.

After considering "*The single spherical surface*" (pp. 229–237 of the presidential address), Mr. Smith then proceeds to discuss problems of similar nature relating to "*The simple lens*" (pp. 237–246), that is, a lens made of some transparent homogeneous substance like glass, whose surfaces are spherical, and which is surrounded by the same medium on both sides. The first surface of the lens is that on which the light falls. The points A_1, A_2 (Fig. 1) where the optical axis or line joining the centres of curvature C_1, C_2 meets the first and second sur-

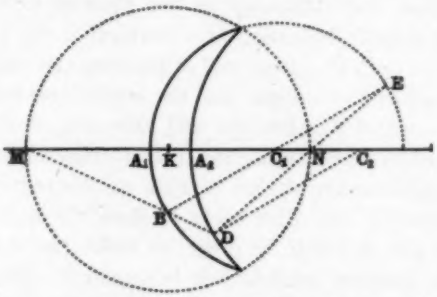

FIG. 1. *Diagram of a crescent-shaped meniscus lens with the centres of curvature of the two surfaces at C_1, C_2 and vertices at A_1, A_2. A straight line drawn through the centre C_1 of the first surface of the lens meets this surface at B; the opposite extremity of the diameter BE being the point marked E. The radius C_2D of the second surface is drawn parallel to C_1B. The optical centre of the lens (which is one of the two centres of similitude of the pair of circles whose arcs are A_1B and A_2D) is M where the straight line BD crosses the optical axis C_1C_2. The other centre of similitude is at N where the straight line DE crosses the optical axis. The dotted circle described on MN as diameter is the section of the harmonic sphere.*

faces of the lens, respectively, are called its vertices; and the axial thickness of the lens is the distance of A_2 from A_1, so that if this magnitude is denoted by d, then $d = A_1A_2$. The radii of curvature, denoted by r_1, r_2, are measured from the vertices to the centres ($r_1 = A_1C_1$, $r_2 = A_2C_2$), each being reckoned as positive or negative according as it is a step in the same direction as that denoted by d or in the opposite direction, respectively. Everything being symmetrical around the

*James P. C. Southall, Conjugate surfaces of a spherical refracting surface. J.O.S.A. & R.S.I., *16*, pp. 380–397, 1928.

optical axis, the form of the lens can be represented by a meridian section made by a plane containing the axis which will intersect each surface in the arc of a circle. Now if the interval C_1C_2 between the centres is divided internally and externally in the ratio of the two radii, the points obtained will be the geometrical centres of similitude of the two circles, and one of them will be the so-called optical centre of the lens, designated here by M; and if the other one of these two points is designated by N, then

$$\frac{C_1M}{C_2M}=\frac{C_1N}{NC_2}=\frac{A_1C_1}{A_2C_2}=\frac{r_1}{r_2};$$

and the distances of M and N from the vertex of the first surface of the lens may be found by the following formulae:

$$A_1M=\frac{r_1d}{r_1-r_2},\quad A_1N=\frac{(2r_2+d)r_1}{r_1+r_2}.$$

Thus the points M, C_1, N and C_2 form a harmonic range of four fixed points on the optical axis of the lens, and, consequently, Mr. Smith calls the sphere described on MN as diameter "the harmonic sphere" (*Presidential Address*, p. 238). If the two surfaces of the lens intersect each other at all, they do so in a circle; and in such a case the harmonic sphere will intersect both surfaces in this same circle. It has certain characteristic properties which, as Mr. Smith takes some pains to show, are useful in studying the optical performance of the lens, but we cannot linger here to comment further on this part of his article.

A very important subject which Mr. Smith proceeds to consider is a practical graphical method of constructing so-called "conjugate secondary surfaces" of a lens with the aid of a chart, as shown in Fig. 20 of his published address, and a piece of tracing cloth that can be rotated over this chart around a pivotal pin. While the process seems to be clever and expeditious, I must confess that it is not altogether clear in my mind, partly perhaps because I have not yet had an opportunity of experimenting with it.

In the following study I have endeavored to solve this same problem in a different fashion. Thus, suppose we concentrate our attention on a certain ray which traverses the lens along a known path, and which is to be considered as the chief ray of a narrow pencil of so-called sagittal rays emanating ("really" or "virtually," as we say in geometrical optics) from a point P on the incident chief ray; the problem consists in constructing the position of this point P (and likewise that of the

conjugate point P′ on the emergent chief ray) for which the magnification-ratio m has a certain prescribed value. If this construction is performed in a meridian plane containing the optical axis for each and every chief ray that is permitted to pass through the lens, two curves will be obtained which are the loci in this plane of the pair of conjugate points P, P′ for which the sagittal magnification-ratio has the required value; and the conjugate surfaces will be generated by revolving these conjugate curves around the optical axis.

2. *The Chief Ray and the Construction of its Path.*—The optical system includes not only the lens itself but a mechanical stop for regulating the apertures of the bundles of effective rays that traverse it. This stop amounts to a plane screen placed at right angles to the optical axis so that the latter passes through the centre O of a small circular hole or diaphragm in the screen. Accordingly, any luminous radiation proceeding from the various parts of the field must go through this tiny opening, either before reaching the lens if the stop is in front of it or after traversing the lens if the stop is on the other side of it. The positive direction along the optical axis being, as above stated, the direction pursued by light in crossing the lens from the vertex A_1 of the first surface to the vertex A_2 of the second surface, the stop is said to be a *front stop* when the step from O to A_1 is in the positive sense as thus defined; whereas it is called a *rear stop* when the step from A_2 to O is positive. When O coincides with A_1, the plane of the front stop is tangent to the first surface of the lens at A_1; and when O coincides with A_2, the plane of the rear stop is tangent to the second surface at A_2. It is theoretically possible—and not impractical under certain circumstances—for the point O to be inside the lens between A_1 and A_2 (*interior stop*), but we need not consider this possibility at present.

Now the *chief ray* of a bundle is that ray which has the distinction of going through the centre of the stop before or after traversing the lens, according as the stop is a front stop or rear stop, respectively. Narrow as the aperture of the bundle must be for all the rays comprised in it to go through the small stop, we shall not consider here the entire bundle, but only one of its two principal sections, namely, the *sagittal section*, as it is called, composed of the pencil of rays that lie in the plane containing the chief ray which is perpendicular to the plane of incidence of this ray. Accordingly, the position of the plane of the sagittal sec-

tion of the bundle will be altered whenever the direction of the chief ray is changed by refraction into another direction; but it remains constantly perpendicular to the fixed plane of incidence of the chief ray.

The lens itself may be considered as a combination of two optical systems each of which is a single spherical refracting surface, and the path of the chief ray inside the lens may be constructed simply by using Young's construction* for a ray refracted at the first surface of the lens; as has been done in Fig. 2, where the straight line RB_1 represents the path of the incident chief ray meeting the first surface of the lens at the point designated by B_1, and the straight line B_1B_2 represents the path pursued by the ray in crossing the lens from B_1 to B_2 where

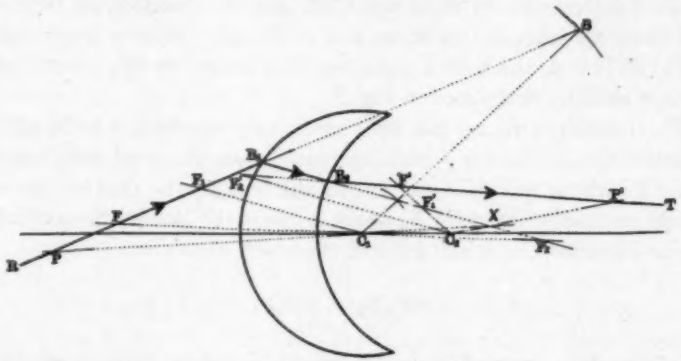

FIG. 2. *Lens surrounded by same medium on both sides showing path RB_1B_2T of the chief ray of a narrow bundle of rays. The position of the focal points F_1, F_1' for the first refraction, F_2, F_2' for the second refraction, and F, F' for the lens as a whole are indicated; and also the positions of a pair of conjugate points P, P'. All these points are shown for the imagery in the sagittal sections corresponding to the three portions of the path of the chief ray.*

it is incident on the second surface. Similarly, the path of the emergent chief ray may be found by using Young's construction for the refraction at the second surface from the lens into the surrounding medium; as shown in the diagram by the straight line B_2T.

3. *The Focal Points F_1, F_1' and F_2, F_2' of the Two Component Optical Systems, and the Focal Lengths f_1, f_1' and f_2, f_2'.*—Assuming, therefore, that the path of the chief ray RB_1B_2T through the lens and into the surrounding medium has thus been constructed, let us proceed now to

*See J. P. C. Southall, *loc. cit.*, p. 384.

locate on it the so-called *focal points* F_1, F_1' for the refraction at the first surface and F_2, F_2' for the refraction at the second surface, since these two pairs of fixed points will be convenient as points of reference. Their positions can readily be found. Through the centre of curvature C_1 of the first surface draw the straight lines C_1F_1 parallel to B_1B_2 and C_1F_1' parallel to RB_1; then the first focal point F_1 for the first refraction will be on the incident chief ray RB_1 where C_1F_1 intersects it, and the second focal point F_1' for the first refraction will be the point of intersection of the straight lines B_1B_2 and C_1F_1'. Similarly, for the second refraction, draw the straight lines C_2F_2 and C_2F_2' through the centre of curvature C_2 of the second surface parallel to B_2T and B_1B_2, respectively; then the first focal point F_2 for the second refraction will be the point of intersection of B_1B_2 and C_2F_2, and the second focal point F_2' will be on the emergent chief ray B_2T at the place where it is crossed by C_2F_2'. (The straight lines C_1F_1' and C_2F_2 used in this construction are not actually delineated in Fig. 2.)

The focal lengths of the two component systems, which will be denoted by f_1, f_1' and f_2, f_2', are measured from the focal points to the point B_1 where the chief ray enters the lens in the case of the first refraction, and to the point B_2 where it leaves the lens in the case of the second refraction; and are defined, therefore, as follows:

$$f_1 = F_1B_1,\ f_1' = F_1'B_1;\ f_2 = F_2B_2,\ f_2' = F_2'B_2.$$

According to a general law of geometrical optics, these magnitudes are related to each other and to the indices of refraction of the media by two simple proportions which may be expressed here as follows:

$$\frac{f_1}{f_1'} = \frac{f_2'}{f_2} = -\frac{n}{n'},$$

where n denotes the index of refraction of the medium surrounding the lens and n′ denotes the index of refraction of the lens-medium itself.

Accordingly, these four focal lengths may be conveniently expressed in terms of two magnitudes D_1, D_2, called the *refracting powers* of the two component optical systems, which are proportional to the reciprocals of the focal lengths and are precisely defined as follows:

$$D_1 = \frac{n}{f_1} = -\frac{n'}{f_1'}, \qquad D_2 = \frac{n'}{f_2} = -\frac{n}{f_2'}.$$

4. *The Focal Points* F, F′ *of the Compound Optical System.*—Let us now consider the compound optical system which is the resultant of the combination of the two component systems of refracting powers D_1 and D_2, separated from each other by the interval B_1B_2 which the chief ray traverses inside the lens. For example, suppose we imagine a point P lying on the chief incident ray RB_1 at a certain distance q from the point of incidence on the first surface ($q = B_1P$), which is the vertex of a narrow pencil of incident sagittal rays all lying close to the chief ray. After the first refraction these rays will all intersect at a point X, let us call it, on the chief refracted ray B_1B_2, which can be readily located because it is the point where the straight line PC_1 drawn through the centre C_1 meets B_1B_2. After being again refracted, this time at the second surface, these rays, having now emerged from the lens, will all intersect once more in a point P′, which is therefore conjugate to P, and which lies on the emergent chief ray of the pencil at a distance from the point B_2 denoted by q' ($q' = B_2P'$). The position of this point can also easily be found by drawing the straight line XC_2 through the centre of curvature C_2 of the second surface which will cross B_2T at P′.

In case the point P′ happened to be the infinitely distant point of the straight line B_2T, as would be the case if XC_2 were parallel to this line, the point P would be identical with the first focal point F of the compound system; and the point X would coincide with F_2. Or, again, if the point P were the infinitely distant point of the straight line R_1B, the straight line joining it with C_1 would be parallel to R_1B, and in this case the point X would be the second focal point F_1' of the first component system; and hence the second focal point F′ of the compound system is the point of intersection of the straight lines $F_1'C_2$ and B_2T. Thus the positions of F and F′ can be found immediately.

5. *The Magnification-Ratio* (m) *in the Sagittal Section, the Refracting Power* (*D*), *and the Image-Equations.*—If a straight line is drawn perpendicular to the incident chief ray at the point P and lying in the plane of the sagittal section, and if a point Q is taken on this line very close to P, the conjugate point Q′ will lie in the plane of the sagittal section of the emergent chief ray on the perpendicular to this ray erected at P′, also very near P′. The *magnification-ratio* for the pair of conjugate points P, P′ is the ratio between these two short perpendiculars, which is denoted by m; that is, $m = P'Q' : PQ$. It may have any value whatever, positive or negative, depending simply on the

position of the point P on the incident chief ray. As long as m is positive, the point P will lie on one side of the first focal point F, and the image of PQ will be erect; whereas for negative values of m the point P will lie on the other side of F, and the image will be inverted. When $m=0$, P will be infinitely far away, and P′ will be at F′; and when $m=\infty$, P will be at F, and P′ will be at infinity.

The refracting power of the optical system, denoted by D, is a magnitude which can easily be computed in terms of the refracting powers D_1, D_2 of the two component systems and the "reduced" interval (t) between them, according to the well-known formula:

$$D=D_1+D_2-t\cdot D_1\cdot D_2,$$

where

$$t=\frac{B_1B_2}{n'}.$$

If the abscissae of the pair of conjugate points P, P′ with respect to the focal points F, F′ are denoted by x, x' respectively, that is if $x=FP$, $x'=F'P'$, the *image-equations* (as they are called) may now be written as follows:

$$\frac{n}{x\cdot D}=-\frac{x'\cdot D}{n}=m,$$

whereby for any given value of the magnification-ratio m, the values of x, x' can be found immediately, and consequently the positions of the corresponding pair of conjugate points P, P′ can be ascertained.

One pair of conjugate points, designated here by U, U′, are so noteworthy that we must pause to speak of them. They are commonly called the *principal points*, but, following Mr. Smith and other English writers, let us call them here the *unit points*, because for this pair of conjugate points the magnification-ratio is positive and equal to unity. If therefore in the image-equations above we put $m=+1$, $x=FU$, $x'=F'U'$, it appears that

$$FU=U'F'=\frac{n}{D};$$

and, consequently, we obtain a geometrical definition of the refracting power D which was defined above simply as an abbreviation for a certain algebraic expression. If, in accordance with our previous notation, the *focal lengths* f, f' of the compound system are defined as follows, in terms of the refracting power:

$$f = -f' = \frac{n}{D}, \text{ or } D = \frac{n}{f} = -\frac{n}{f'},$$

then $f = FU$ and $f' = F'U'$; that is, the focal lengths are the distances of the unit points from their corresponding focal points.

All this, of course, is nothing new, and must seem very familiar to the student of geometrical optics. However, no apology is necessary for re-stating these facts in order to explain distinctly the system of notation that is employed here, even if there were no other reason. The positions of the focal points and unit points with respect to the points B_1 and B_2, where the chief ray enters the lens and leaves it, are given by the following formulae for the combination of two optical systems:

$$\frac{B_1U}{n} = \frac{D_2}{D}t, \qquad \frac{B_2U'}{n} = -\frac{D_1}{D}t;$$

$$\frac{B_1F}{n} = -\frac{1 - t \cdot D_2}{D}, \quad \frac{B_2F'}{n} = \frac{1 - t \cdot D_1}{D}.$$

6. *Graphical Construction of the Focal Lengths f and f' of the Compound Optical System.*—The formulae given above enable us to calculate the various magnitudes and to find the abscissae x, x' of the pair of conjugate points for which the magnification-ratio has the prescribed value m; but this is not the solution of our problem, which was to construct geometrically the positions of the points P and P'. There is no difficulty, as we have seen, about constructing the path of the chief ray through the lens and the positions of the focal points F_1, F_1'; F_2, F_2'; and F, F'. But we cannot proceed further until we know how to construct the focal lengths f, f' or, what comes to the same thing, the positions of the unit points U, U'. Accordingly, let us show how this may be done by an auxiliary geometrical construction. The actual process, it may be remarked, is much shorter than the explanation of it.

In the accompanying diagram (Fig. 3), Ox and Oy are the positive directions of two straight lines drawn from a point O, and the points A, B_1 and C are taken on Ox so that $OA = -f_2'$, $AB_1 = -nt$, and $B_1C = -f_1$; that is $AO = f_2'$, $B_1A = nt$, $CB_1 = f_1$. Next, mark the point D on Oy such that $OD = OA$, complete the parallelogram B_1ODE, and draw the diagonal B_1D. Through the point H where this diagonal meets the straight line CE, draw FG parallel to Oy intersecting Ox in F and DE in G; and, finally, mark the point U on Ox such the $FU = FH$.

Then the points B_1, F and U will be ranged along Ox exactly in the same way as the points designated by these letters are ranged along the

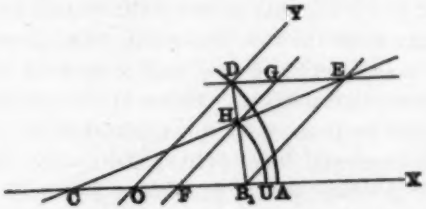

FIG. 3. *Auxiliary diagram for construction of first focal point F, first unit point U, and first focal length f = FU.*

incident chief ray, and $FU = f$. The proof of the construction consists in showing that the formulae for calculating the positions of these points can be derived from the figure by considering the two pairs of similar triangles HDE, HB_1C and B_1FH, B_1OD; as the reader can easily verify.

The positions of the points F′ and U′ on the emergent chief ray may be found by a similar geometrical construction, as shown in Fig. 4, where O′x′, O′y′ are the positive directions of two straight lines drawn through a point O′. On O′x′ the points A′, B_2 and C′ are taken so that

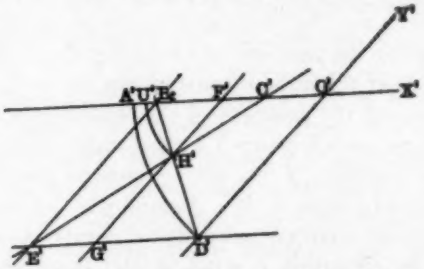

FIG. 4. *Auxiliary diagram for construction of second focal point F′, second unit point U′, and second focal length f′ = F′U′.*

$O'A' = (n/n')f_1'$, $A'B_2 = nt$, and $B_2C' = (n/n') \cdot f_2$; and the point D′ is marked on O′y′ such that $O'D' = O'A'$. Then the parallelogram $B_2O'D'E'$ is completed, the diagonal B_2D' drawn to meet the straight line C′E′ in H′, and through H′ the straight line F′G′ drawn to meet O′x′ in F′ and D′E′ in G′. Finally, the point U′ is marked on O′x′ such that $F'U' = F'H'$. If this figure is properly constructed, the points B_2, F′ and U′ will be ranged along the straight line O′x′ in exactly the same

way as the points designated by these letters are ranged along the emergent chief ray, and $F'U' = f'$. The proof, which likewise is similar to the proof of the other construction, can be deduced immediately from the two pairs of similar triangles $H'D'E'$, $H'B_2C'$ and $B_2F'H'$, $B_2O'D'$.

7. *Construction of the Pair of Conjugate Points* P,P′ *corresponding to a given value of the Magnification-Ratio* m.—As a matter of fact, it is not necessary to perform the construction given above for the second focal length f' of the compound system; for, if the first focal length f has been found by the first of the two constructions, then since

$$FP = \frac{f}{m},$$

all we have to do to find the point P (Fig. 2) is to lay off on the incident chief ray RB_1 the step FP equal to one-mth of the first focal length, and then construct P′ by drawing PC_1 meeting B_1B_2 in X and XC_2 meeting the emergent chief ray B_2T in the required point P′ conjugate to P.

After all, let me hasten to say, there is nothing essentially new about the construction which has been outlined in the preceding pages, and the reader may be disappointed to find that he has simply applied the well-known laws of geometrical optics for the combination of two optical instruments. For example, the whole process could perhaps have been deduced from some earlier work such as Lippich's elegant paper on collineaf relations between narrow bundles of rays published a half-century ago.* Moreover, while there is no particular difficulty in performing the various operations, beginning with the construction of the path of the chief ray, and including the location of the focal points and finding the focal lengths of both the two component optical systems and the compound system, it all takes some little time, and the whole process has to be repeated for each chief ray concerned, in order to locate the positions of all the pairs of conjugate points P, P′ for which the magnification-ratio has the prescribed value. On the contrary, Mr. Smith implies that the method with chart and tracing cloth, as described on pages 241–244 of his published address, to which I have referred already, is easy and convenient; indeed, he says that, after the "chart" has been made, "a complete surface may be traced in this way with good accuracy in less than a minute."

*F. Lippich, Über Brechung und Reflexion unendlich dünner Strahlensysteme an Kugelflächen. Denkschriften der kaiserl. Akad. der Wissenschaften zu Wien, *38*, pp. 163–192; 1878.

Obviously, no general method of constructing the conjugate secondary surfaces of a lens can be devised that will be nearly so simple as the solution of the same problem for the case of a single spherical refracting surface, as found in my previous paper above referred to. However, let us see whether that process can be conveniently adapted to the case of a lens. If m_1, m_2 denote the magnification-ratios for the two surfaces of the lens, obviously, the product of these magnitudes must be equal to the total magnification-ratio of the compound optical system, that is,

$$m = m_1 \cdot m_2;$$

and it may be shown without difficulty that

$$m_1 = \frac{m \cdot D}{D_1 + m \cdot D_2}.$$

While this expression is convenient for calculating the required value of the magnification-ratio m_1 of the anterior part of the compound system in terms of the given value of m and the refracting powers D_1, D_2 of the two component systems, it may be put in a form that is more suitable for the determination of m_1 by geometrical construction, namely,

$$m_1 = \frac{F_1'F_2}{F_1'B_1 - \frac{F_2B_2}{m}}.$$

Since each of the fixed intervals $F_1'F_2$, $F_1'B_1$, and F_2B_2 can be plotted in an auxiliary diagram, a simple geometrical process can be devised for finding the value of the ratio m_1. This being done, the subsequent procedure consists merely in finding the required point P by the method given in my previous paper for the case of a single spherical refracting surface, namely, as follows: Draw the normal to the first surface of the lens at the incidence-point B_1 (Fig. 5), mark on it the position of the point Z, such that $B_1Z = a$, and around Z as centre with radius $ZP = k$ describe the arc of a circle cutting the incident chief ray in the point P; the magnitudes denoted here by a and k being defined as follows:

$$a = \frac{1 - m_1}{m_1} \cdot \frac{n^2}{n'^2 - n^2} \cdot r_1, \quad k = \frac{n'}{n} a.$$

The point marked S in Fig. 5 is found (as in Young's construction of a ray refracted at a spherical surface) by describing the arc of a circle

around C_1 as centre with radius equal to $(n'/n)\, r_1$ which will cut the straight line RB_1 at S; and it will be seen that the triangles B_1CS and B_1ZP are similar, and therefore

$$\frac{B_1P}{B_1S}=\frac{a}{r_1};$$

so that the point P may be constructed in this way provided the value of the ratio

$$\frac{a}{r_1}=\frac{1-m_1}{m_1}\cdot\frac{n^2}{n'^2-n^2}$$

is known in advance.

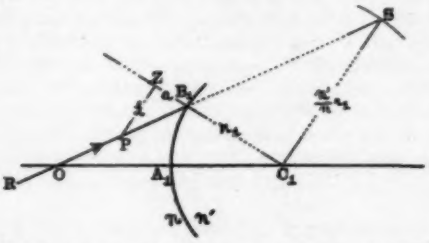

FIG. 5. *First surface of lens, showing ray incident on it, and construction of point P corresponding to a given value of the magnification-ratio* m.

It may be questioned whether either of the two methods of finding the positions of the pair of conjugate points P and P′, which I have outlined above, is a strictly geometrical process of construction, as I myself am well aware. Both methods are obviously based on analytical considerations. It should be borne in mind, however, that I have sought to discover a general method that would be applicable to all cases; and whether I have succeeded or not, I can claim at least that the inherent factors in the problem have been exposed to view; and I am convinced that these factors will be encountered in some form or other, no matter what method is pursued or how ingenious it may appear to be at first sight.

Attention might be called to some special cases, as, for example, when the thickness of the lens is negligible or when one of its surfaces is flat, but the reader can easily investigate these for himself.

Obviously, the process described above for the case of a single lens surrounded by the same medium on both sides can be extended without much difficulty to the general case of an optical system composed of a centered system of more than two spherical refracting surfaces;

although the number of necessary steps in the construction will be correspondingly increased.

In conclusion, I wish to thank my colleague, Mr. C. L. Treleaven, for his aid in drawing the figures that have been used to illustrate this paper.

COLUMBIA UNIVERSITY,
DEPARTMENT OF PHYSICS.
APRIL 10, 1928.

THE PENETRATION OF ULTRAVIOLET LIGHT INTO PURE WATER AND SEA WATER*

By E. O. Hulburt

ABSTRACT

With a quartz spectrograph, sodium hydride quartz photoelectric cell and quadrant electrometer, measurements were made in the ultraviolet spectrum region λ4000 to 2500A of the light absorption coefficients of pure water and sea water and of the molecular absorption coefficients of aqueous solutions of the principle salts in the sea, namely, NaCl, KCl, $MgCl_2$, $MgSO_4$ and $CaSO_4$. The transparency of the sea water declines rapidly with decreasing wave length in the ultraviolet becoming quite small below λ3000A. From λ3400 to 3000A, $CaSO_4$ contributes about half to the absorption of sea water, H_2O about a fourth and the other salts the rest; from λ3000 to 2500A, $MgCl_2$, $CaSO_4$ and H_2O each contribute roughly a third, the other salts giving relatively little absorption. There is a close correspondence between the falling off in the transparency of the sea with decreasing wave length in the ultra violet and the spectral energy curve of sunlight. This, together with the very similar correspondence in the case of the transparency of the atmosphere permits the suggestion that the actinic effects of sunlight may have played a part, perhaps more important than has been heretofore recognized, in the constitution of the sea and the air.

No records appear to be available of measurements of the penetration of ultraviolet light into the water of the ocean. In the present investigation the absorption coefficients in the region of λ4000 to

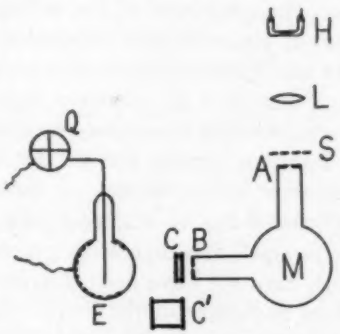

Fig. 1. *Diagram of apparatus.*

2500A have been determined for pure water, sea water and for aqueous solutions of the principal salts in the sea, namely, the chlorides of sodium, potassium and magnesium, and the sulphates of magnesium and calcium.

* Published with the permission of the Navy Department.

The light from a small quartz mercury lamp H, Fig. 1, filled with mercury at a pressure of about one and a half atmospheres, taking 2 amperes D.C. at 70 volts, was focused by a quartz lens L on the slit A of a quartz monochromatic illuminator M (Hilger, Type D33). The approximately monochromatic beam of light from the second slit B passed through the absorption cells C or C' and fell into the quartz sodium hydride photoelectric cell E. The cell E was connected, by means of a suitably insulated and shielded wire with an earthing key, to a Compton quadrant electrometer Q of sensitivity about 1000 mm deflection per volt difference of potential between the quadrants. The light was turned on for known intervals of time by a shutter S electrically operated by a pendulum of three seconds period. The two cells, C and C', just alike except that one was thin and the other thick, were filled with the liquid whose absorption was to be examined and were placed in turn behind slit B. The cells were made of a short tube of Pyrex glass, of inside diameter 2 cms, with the ends carefully ground to flatness and closed with plane quartz plates; no cement was used. One cell was 2.07 cm long and the other 0.15 cm.

Measurements were made with the strong ultraviolet mercury lines, the slits A and B being opened to a suitable width sometimes less than 1A, never more than 10A, for each line, depending upon the intensity of the line. The sensitivity of the sodium hydride cell rose to a broad maximum at about λ3650A, descended rapidly to a minimum around λ2700A and increased again at shorter wave lengths. As a result there was a correction for scattered light for wave lengths below 3000A. This was carefully determined by means of observations with a clear glass absorbing screen, but as the liquids investigated were all fairly transparent in the thicknesses used the corrections of the absorption coefficients due to scattered light, although always made, turned out to be small, less than a few percent. It was thought that any errors which may not have been eliminated were more probably due to chemical impurities of the liquids than to faulty measurements. The electrometer deflections were accurate to less than 2% and the absorption coefficients were correct within 10 to 20%, the possible error being greater than this for the very small coefficients.

For a specified wave length the *light absorption coefficient* α of a liquid is defined by the relation

$$I = I_0 10^{-\alpha x}, \tag{1}$$

where I_0 is the original intensity of the light and I the intensity after passing through x cms of the liquid. If d and d' were the electro-

meter deflections for the cells of thickness x and x', respectively, $\alpha = (log_{10} d/d')/(x'-x)$. The measurements of the solutions have been recorded as the *molecular absorption coefficient* A. This is defined by

$$A = (\alpha - \alpha_0)/c, \qquad (2)$$

where α is the absorption coefficient of the solution, α_0 of the pure solvent (in the present case, water), and c is the concentration in gram-molecules per liter of solution. This definition, which is the usual one, assumes that the absorption of a solution is the sum of two parts, the first due to the salt and the second to the pure solvent, and that the absorption due to the solvent is the same as it would be if there were no dissolved salt present.

TABLE 1. *Value of α for water and sea water and of A for aqueous solutions of the principal salts in the sea water.*

	α			A				
λ in mμ	distilled water	tap water	sea water	NaCl	KCl	$MgCl_2$	$MgSO_4$	$CaSO_4$
254	0.030	0.045	0.067	0.0045	0.0123	0.453	0	1.98
266	0.021	0.032	0.057	0.0047	0.0104	0.240	0	1.84
280	0.015	0.020	0.039	0.0024	0.0080	0.154	0.0005	1.91
289	—	—	—	—	0.0048	0.043	—	—
303	0.005	0.007	0.017	0.0019	0.0041	0.021	0.0041	1.12
313	0.002	0.003	0.009	0.0015	0.0035	0.012	0.0078	0.613
366	0.001	0.001	0.0013	0.00016	0.0019	0.0031	0.0046	0.000
436	0.00005		0.00010					
546	0.000148		0.00015					
578	0.000278		0.0003					
612	0.0010		0.0010					

The values of α for water doubly distilled in Pyrex are given in the second column of Table 1 and are in curve 1, Fig. 2. The water was distilled a third time in Pyrex, a fourth time in quartz and was allowed to flow directly into the cells. The absorption coefficients of this water agreed within the error of measurement with the values of column 2. In Table 1 are also given the pure water values of α for the visible wavelengths 436, 546 and 578mμ from Martin[1] and 612mμ from Auf-

[1] Martin Journ. Phys. Chem., *26*, p. 471; 1922.

sess.[2] The values of α for tap water are in the third column of the table and are plotted in curve 2, Fig. 2. The tap water contained traces of iron and probably other impurities. Kreusler[3] has given a table of the ultraviolet absorption coefficients of pure water which is copied into Landolt-Börnstein (*2, p.* 896, Table 164C, 1923) and into the Smithsonian Physical Tables (7th Edition, p. 307, Table 376, 1927). His values of α are ten times lower than those calculated from the original measurements given in his paper (assuming no misprints in his original measurements). Multiplying his values of α by 10 and interpolating among them to get α for the wave lengths of Table 1 gives α to be 0.013, 0.012, 0.010 and 0.006 for λ254, 266, 280 and 303mμ, respectively. These agree none too well with the measurements of Table 1.

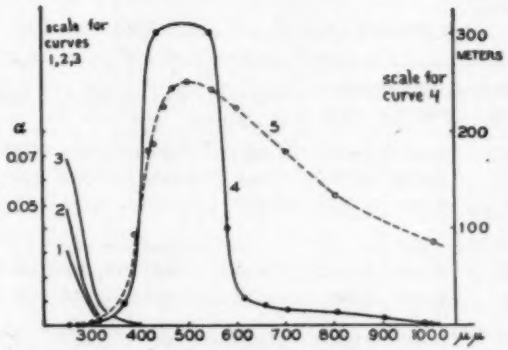

FIG. 2. *Curves 1, 2 and 3 are the absorption coefficients α for pure water, tap water and sea water, respectively. Curve 4 is the distance light penetrates into the sea to be reduced to 1/1000th in intensity. Curve 5 is the spectral energy curve of sunlight plotted with ordinates in arbitrary units.*

In curve 5, Fig. 1, of a former paper[4] Kreusler's ultraviolet values of α for water were used in part of a calculation of the spectral intensity curve of Palaeozoic daylight. If the present values of α for pure water, or for sea water, Table 1, column 4, were used instead of those of Kreusler, the Palaeozoic daylight curve would resemble even more closely the visibility curve of the eye. Further, Kreusler's values of α are within a factor of 4, throughout the range λ3600 to 2000A, of

[2] Aufsess, Ann. d. Phys., *13*, 1904.
[3] Kreusler, Ann. d. Phys., *6*, p. 412; 1901.
[4] Hulburt, J.O.S.A., & R.S.I. *13*, p. 553; 1926.

the absorption coefficients of water calculated from Raman's[5] extension of the Einstein-Smoluchowski theory of molecular diffraction, but if Kreusler's values are wrong this very good agreement with theory in the ultraviolet unfortunately disappears. The agreement with Raman's theory for visible light remains untouched of course in any case, and Raman's attractive explanation of the color of the sea on the basis of molecular scattering is undisturbed.

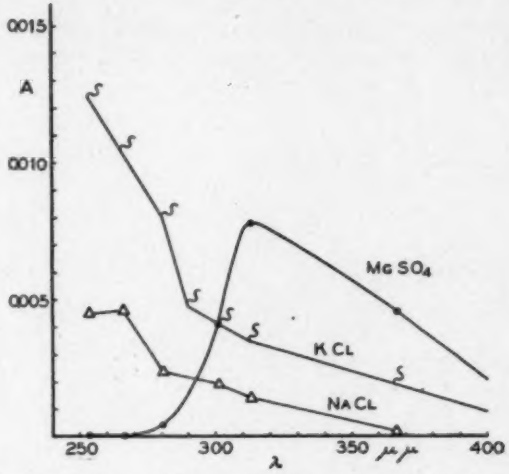

FIG. 3. *Molecular absorption coefficient A of $MgSO_4$, KCl and NaCl in aqueous solution.*

In one liter of water of the ocean there are[6] 26.4, 0.75, 3.15, 2.07 and 1.33 grams of NaCl, KCl, $MgCl_2$, $MgSO_4$, and $CaSO_4$, respectively, with traces of other salts, such as 0.005 grams of $FeCO_3$, etc. The absorption coefficients of aqueous solutions of these five salts of known concentration (about three fourths saturated) were measured and the molecular absorption coefficients A were calculated from (2); these are given in the last five columns of Table 1 and are plotted in Figs. 3 and 4. The values for $MgCl_2$ agree very poorly with the measurements of Getman[7] for this salt. The salts were fairly pure according to Baker's analysis; they contained for the most part traces of each other

[5] Raman, Proc. Roy. Soc., *101*, p. 64; 1922. "Molecular Diffraction of Light," Calcutta University Press, 1922.

[6] Thorpe, "Dictionary of Applied Chemistry," 7, p. 379; 1927. Clark, "The Data of Geochemistry," Bull. 770, U. S. Geological Survey, 1924.

[7] Getman, Journ. Phys. Chem. 29, 853 (1925).

as impurities, and in the case of the NaCl and the $MgSO_4$ there was 0.001% of iron. From the values of A for the salts and of α for pure water, the values of α for sea water were calculated and are given in the fourth column of Table 7; they are plotted in curve 3, Fig. 2. Artifical sea water made with the five salts in proper proportion gave absorption coefficients 5 to 10% greater than those in column 4. This fair agreement with the values calculated from the molecular absorption coefficients of the separate salts showed that A was a constant when the concentration was varied. This is Beer's "law," which is known[8] to hold tolerably well for aqueous solutions in those regions of the spec-

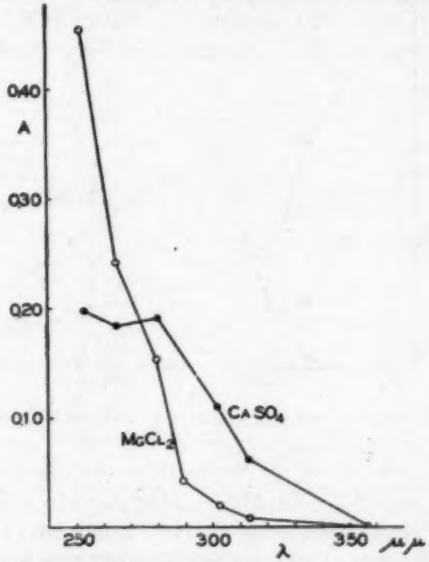

FIG. 4. *Molecular absorption coefficient A of $MgCl_2$ and $CaSO_4$ in aqueous solution. For the $CaSO_4$ curve the ordinate scale must be multiplied by 10.*

trum where the absoption is small, as is the case here. Actually, measurements were made on solutions of $MgCl_2$ of varying concentrations for λ265, 280 and 289mμ, this being the only salt which possessed much absorption, and Beer's law was found to hold within the error of measurement.

Samples of sea water taken about two months ago from the Gulf Stream and from the Caribbean Sea far from land gave absorption coefficients in close agreement with those in Column 4, Table 1, for

[8] Hulburt and Hutchinson, Carnegie Instit. Pub., 260; 1918.

the wave lengths longer than 300mμ; for wave-lengths below 300mμ the sea water values were about 20% greater than those of the table. On the whole we may take the values of α in column 4 as being not far from those of the water of the open sea. The values of α in the visible spectrum for sea water given in column 4 were taken from an earlier investigation.[4] It is seen that the transparency of the sea declines rapidly with decreasing wave length in the ultraviolet becoming quite small below λ3000A. From λ3400 to 3000A $CaSO_4$ contributes about half to the absorption of sea water, H_2O about a fourth and the other salts the rest; from λ3000 to 2500A $MgCl_2$, $CaSO_4$ and H_2O each contribute roughly a third, the other salts giving relatively little absorption.

The distances, calculated from the absorption coefficients, which light of various wave lengths penetrates intothe ocean to be reduced to 1/1000th of its original intensity are given in curve 4, Fig. 2. Curve 5 is the observed energy distribution of sunlight,[9] the ordinates of the curve are in arbitrary units. We notice that the transparency of the sea falls off with the wavelength in the ultraviolet just as the spectral energy of the sun does, the sea being very transparent for those wave lengths of sunlight which are strong and opaque to the weak ones (assuming that the black body energy curve of the sunlight may be extrapolated into the ultraviolet). This reminds us very much of the transmission of the atmosphere of the earth in clear weather which begins to decrease appreciably at λ3900A and falls to zero at about 2900A because of the strong absorption of ozone in the high atmosphere. In Fig. 5 are given spectrograms which illustrate the similarity: strips *a* and *f* are spectra of the direct quartz mercury arc; strip *b* is the mercury spectrum after passing through a tube of artificial concentrated sea water equivalent to 10 meters of natural sea water (by calculation from the known concentrations and absorption coefficients of the salts); strip *c* is the solar spectrum; and strips *d* and *e* are the mercury spectrum after passing through 2.07 cm and 0.15 cm, respectively, of a saturated aqueous solution of $MgCl_2$.

It is difficult to regard as a coincidence the facts that the atmosphere of the earth and the water of the sea are very transparent to the most intense spectral regions of sunlight, i.e. around λ5000A, and fall off in transparency in the ultraviolet much as the solar spectral energy curve does. It seems more reasonable to suppose that the part

[9] Abbott, Fowle and Aldrich, Annals of the Astrophysical Observatory of the Smithsonian Institution, *3*, p. 197; 1913.

played by the sun's ultraviolet light in the constitution of the air and oceans has not been inappreciable, especially since photoelectric, photochemical, etc., effects are prominent for the ultraviolet wave lengths. In the infrared, such close correspondence would not be expected, because of the relative absence of actinic effects at these wave lengths, nor does it exist, the sea water becoming opaque at about 1μ, the atmosphere at about 4μ, and there being considerable energy (calculated) in the sunlight beyond these wave lengths. The hypothesis that one comes to, to put it graphically (and no doubt much too extremely), is that the strong wave lengths of the sunlight

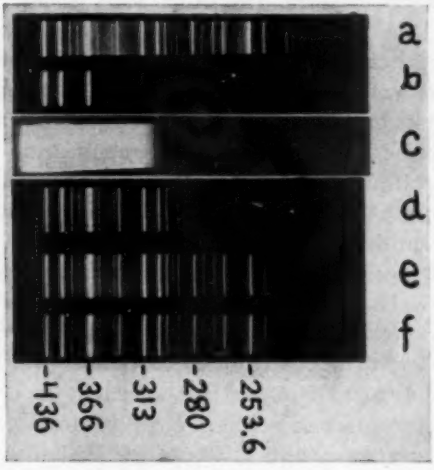

FIG. 5. *a and f direct mercury arc; b mercury arc through concentrated artificial sea water equivalent to 10 meters of natural sea water; c solar spectrum; d and e mercury arc through 2.07 cm and 0.15 cm, respectively, of a saturated aqueous solution of* $MgCl_2$.

have literally burned their way through the atmosphere and into the sea, helping to destroy and to disperse substances which may have impeded them, and, more graphically, that sodium chloride remains in the sea and nitrogen in the atmosphere because, in part, they are transparent to the energetic waves of the solar spectrum and that copper sulphate is not in the sea nor chlorine in the atmosphere (the choice of illustrations may turn out to be unfortunate, but no matter) because they are opaque to these waves.

NAVAL RESEARCH LABORATORY,
WASHINGTON, D. C.
APRIL 6, 1927.

THE ULTRAVIOLET, VISIBLE AND INFRARED REFLECTIVITIES OF SNOW, SAND AND OTHER SUBSTANCES*

By E. O. Hulburt

ABSTRACT

By means of a quartz mercury lamp, a thermocouple and absorbing screens, the diffuse reflectivities in the region λ0.3 to 7μ were measured for snow, sand, crushed quartz, plaster paris, white paper, white cotton cloth, sodium carbonate and sodium chloride. The ultraviolet reflectivity of snow was relatively high, being two to four times that of sand. This gives a physical basis for the current idea that ultraviolet glare may be an important factor in snow blindness.

The reflectivities for regions of the spectrum from λ300mμ to 7μ have been determined for a number of diffuse reflecting materials, such as snow, sand, white cotton cloth, sodium chloride, etc. The substance under examination was laid or placed in a tray 20×25 cm, at *S*, Fig. 1. The light from a small quartz mercury lamp *H* diffusely reflected from the substance fell upon the thermocouple *T* which was conected to a galvanometer. *H* and *T* were 25 cms above *S* and were 18 cms from each other. A shutter *A* turned on and off the light and at *B* various absorption screens were placed; diaphragms and opaque screens kept extraneous light from the thermocouple.

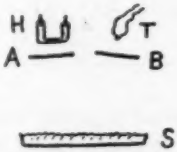

FIG. 1. *Arrangement of apparatus.*

Five absorbing screens were used for separating out various spectral regions, quartz, a water cell with quartz ends, clear glass, Corning "Heat Transmitting Glass" and Corning "Corex" glass. The transmission curves of these were carefully determined throughout the spectral region from λ2500A to 6μ with ultraviolet, visible and infrared spectrophotometers. The distribution of energy in the spectrum of the mercury lamp was also determined. The lamp was a small one of quartz filled with mercury vapor at about one and a quarter atmos-

* Published with the permission of the Navy Department.

pheres pressure taking 70 volts and 3 amperes direct current. The relative energies in the regions $0.25-0.4\mu$, $0.4-0.8\mu$, $0.8-2.6\mu$, $2.6-7\mu$ and beyond 7μ were 5.3, 9.4, 16.9, 18.1 and 50.3, respectively. For the first region the energy was largely in the line groups at 302, 312 and 366mμ, for the second in the blue green and yellow lines, for the last three regions the energy probably owed its character more to the radiation from the hot quartz, etc., than to the mercury vapor. The values of the reflecting power were considered to be correct within 10%. Instrumental errors, due mainly to unsteadiness in the thermocouple caused by temperature changes in its surroundings, were fairly small. Some uncertainty may exist in the values for the visible part of the spectrum because these were obtained by subtracting the reflections in the other parts of the spectrum from the total reflected radiation, a method which is permissible, but only approximately so, where there are no very marked bands of selective reflection, as was the case here.

TABLE 1. *Diffuse reflecting powers in relative units*

Spectral region	Maine sand	Florida sand	Crushed quartz	Snow	Plaster of paris	White paper	Sodium carbonate	Sodium chloride	White cotton cloth
0.3–0.4μ	8	15	40	35	40	8	14	38	36
0.4–0.8	25	40	50	40	53	30	28	49	42
0.8–2.6	33	50	53	15	60	30	35	54	40
2.6–7	31	30	28	18	63	15	18	55	20
7 –	48	—	—	26	—	—	—	—	—

The diffuse reflecting powers of a number of materials are given in relative units in Table 1. Because there was relatively little energy in the mercury spectrum below 0.3μ the ultraviolet region has been given in the table as 0.3–0.4μ, although the Corex filter was fairly transparent as far as $\lambda 0.26\mu$. The sand from the seashore of Maine was made up of grains of many colors, such as clear, white, yellow, gray, red, etc., and as a whole was yellow white in color. The Florida sand came from two miles inland from the sea and was very white, containing quartz with some black specks. The crushed quartz was made by grinding clear optical quartz in a mortar, its grains were irregular in size. The snow was an untouched surface of freshly fallen snow in a tray. The plaster of paris was in powder form; the white paper was very slightly yellowish; the sodium carbonate was

anhydrous; the white cotton cloth was an old handkerchief freshly washed and ironed. No attempt was made to carry out a complete investigation of the reflectivities of diffuse reflecting surfaces, but it might be remarked that powdered quartz in a sufficiently thick layer would be expected to be the perfect diffusing surface for the visible and ultraviolet regions of the spectrum; the size of the particles might have to be considered.

The reflectivities of snow and sand are of particular interest (indeed, the present investigation germinated from this). For heat radiation the sand has a high reflectivity and no doubt contributes not a little to the heat of a desert, which is probably hot enough already. Contrariwise, the poor heat reflectivity of snow brings little comfort in the cold surroundings of a winter day. The ultraviolet reflectivity of snow is relatively high, being two to four times that of sand. Spectrograms of the mercury light scattered back from snow and sand showed qualitatively that the reflectivity of the snow, although falling off with the wave length, continued to gain on that of sand down to $\lambda 210 m\mu$. It has recently been found[1] that the ratio of the ultraviolet to the visible light of the sun is greater in far northern latitudes (Lapland) and on high mountains (the Jungfrau) than in temperate zones (Germany). These facts indicate that ultraviolet glare is perhaps an important factor in snowblindness. There is of course nothing novel in this, but the evidence on the physical side seems now more definite.

NAVAL RESEARCH LABORATORY,
WASHINGTON, D. C.
APRIL 11, 1928.

[1] Kestner, Naturwiss., *44*, p. 879; 1927.

ON THE THEORY OF FORCED DOUBLE REFRACTION (PHOTOELASTICITY)

By K. F. Herzfeld

ABSTRACT

The double refraction of crystals may be due (1) to anisotropy of the ions taken separately; (2) to the anisotropic arrangement of the ions in the lattice, which results in an anisotropic force even if the ions are undisturbed; (3) to an anisotropic Lorentz-Lorenz force due to the anisotropic arrangement of the ions. Ewald and Bragg have assumed (3) alone to be present. Here calculations are made for effect (3) in cubic crystals under stress (forced double refraction, photo-elasticity). The effect seems not to be explained entirely by (3). Incidentally it is shown how the Lorentz-Lorenz force is built up in the unstrained crystal. It turns out that the force $-4\pi P+4\pi/3P$ is almost entirely due to the plane passing through the considered ion.

1. INTRODUCTION

Noncubic crystals are double refracting. The question arises, if this double-refractivity can be explained entirely by the arrangement of the ions (or atoms) in the crystal-lattice, assuming each ion itself to be isotropic, or if part of the effect must be ascribed to an anisotropy of the ion itself.

Furthermore, in the first case, the action may be of two kinds. The noncubic arrangements of the ions in the neighborhood may result in a different force, in different directions, even if the surrounding ions are not polarized themselves, this force being due to their charges in their undisturbed positions. Or, it might be that only the Lorentz-Lorenz force were anisotropic, the force which originates in the fact that the surrounding ions are also polarized by the same external homogeneous field.

First, Ewald[1] tried to answer this question at a time when the exact lattices were not known. So he could show in the case of anhydrite only, that the order of magnitude came out right if he assumed the double refraction to be due entirely to the Lorentz-Lorenz force. His method was applied by Heine[2] to the problem of forced double refraction in an unpublished thesis. Next Bragg[3] made calculations for a number of carbonates, nitrates and for alum under the same assumptions.

[1] P. P. Ewald, Thesis, Munich, 1912, Ann. d. Phys., *49*, p. 1; 1916.
[2] W. Heine, Thesis, Munich, 1922.
[3] W. L. Bragg, Proc. Roy. Soc. A., *105*, p. 370; 1924; *106*, p. 346; 1924.

Hylleraas[4] calculated the double refraction of Hg_2Cl_2, Hg_2Br_2 and quartz, calculating at the same time the optical activity. He not only took into account the Lorentz-Lorenz force, but also the forces due to the non-cubical arrangement of charges in the neighborhood. Both Bragg and Hylleraas succeeded to get the experimental values for the double refraction, but Hylleraas could adjust the otherwise unknown values of the ionic refractivities themselves so as to fit the experiments.

It is well known that isotropic substances, subjected to strain, become double refracting. This effect is widely applied in measuring stresses in workpieces of complicated form; celluloid, made in the same form, is subjected to the corresponding strains and the distribution of double-refraction observed. (Photo-elasticity.) If one applies to a piece of a simple cubic crystal like rocksalt a uniform strain, one can easily calculate the geometric change in the lattice, and as in this case the refractivities of the ions are known in the undeformed state, the amount of double refraction, which is due to the change in lattice alone, can easily be calculated and compared with the measurements. The latter were first performed by Pockels[5] and repeated by Mr. Maris[6] in the Naval Research Laboratory in Washington, D. C., for different wave lengths.

The result is that the calculated effect is different from the observed, pointing to effects either corresponding to (1) or (2).

2. THE EFFECT OF LATTICE CHANGES

To make the influence of the arrangement of resonators in the lattice physically clear, we must give a short review of the formal theory of dielectrics, and of the derivation of the so-called "Lorentz-Lorenz force."

(a) *Uniform medium.* In a condenser in vacuum the electric field is equal to the displacement D, which is determined by the true charges on the plates. If we now fill the condenser with a dielectric and consider the force on the charge inside of a spherical cavity in the medium, we can reason in the following way: The medium is under this circumstance homogeneously polarized with a polarization $4\pi P = N4\pi p$, if N is the number of particles in 1 cm³ and p the electrical moment of one particle. The forces in the cavity can be attributed to the action

[4] E. Hylleraas, ZS. f. Ph., *36*, p. 859; 1926; *44*, p. 871; 1927.
[5] F. Pockels, Ann. d. Phys., *39*, p. 440; 1890.
[6] H. B. Maris, J.O.S.A. & R.S.I., *15*, p. 194; 1927.

first, of the true charges on the plates, secondly to the induced charges on the surfaces of the medium. The first part is equal to D, the second consists again of two parts, namely the action from the two plane parallel boundaries of the medium, result $-4\pi P$ (charges opposite to the true charges, therefore $-$) and the action from the surface of the cavity, $+(4\pi/3)P$ (Lorentz-Lorenz force, same sign as external effect). If the molecule gets a polarization

$$p=\frac{3r}{4\pi} \tag{1}$$

under the influence of a force 1, we have

$$p=\frac{3r}{4\pi}\left(D-4\pi P+\frac{4\pi}{3}P\right)=\frac{3r}{4\pi}D\left(1-\frac{n^2-1}{n^2}+\frac{n^2-1}{3n^2}\right)$$
$$=\frac{3r}{4\pi}D\left(1-\frac{2}{3}\frac{n^2-1}{n^2}\right)$$

with $P=$ p$\times$number of particles in 1cm^3 and

$$\frac{n^2-1}{n^2}=\frac{4\pi P}{D} \tag{3}$$

n being the index of refraction. This leads to the usual formula.

(b) *Simple cubic lattice.* In a simple cubic lattice we get the same result. We will deduce it here in detail, because we can then better understand how the result comes about. We are allowed to use the electrostatic calculation also for optical purposes, because according to Born,[7] the double refraction is determined by the zero order in the development of the polarization in a power-series of a/λ, a being the lattice distance.

We assume a simple cubic lattice, lattice points at the coordinates $x=al$, $y=am$, $z=an$, l m n all integers. In each lattice point there is a dipole of moment p, parallel to z. The question is, what will be the value of the field at the point $x=y=z=0$ (apart from the field due to the dipole 000 itself). There are three methods to calculate this, one consists in using formulas of Appell[8] and Madelung,[9] the others were given by Ewald[10] and Born.[11] We will use the first, because it shows in the clearest way the influence of each part of the lattice.

[7] M. Born, Dynamik der Kristallgitter, Leipzig, 1923.

[8] P. Appell, Acta math., *4*, p. 313; 1884; *8*, p. 265; 1886; Jour de math., *3*, p. 5; 1884; Pal. Rend., *22*, p. 361; 1906.

[9] E. Madelung, Phys. ZS., *19*, p. 526; 1918.

[10] P. P. Ewald, Ann. d. Phys., *49*, p. 1; 1916.

[11] M. Born, l.c.

Madelung gives the potential due to equal charges in the lattice-points. We want the z-component of the force due to dipoles polarized parallel to z. We must then differentiate Madelung's formulas twice in respect to z and replace the charge E by the moment of a dipole p. Madelung builds up the potential by steps. First we consider the field due to the points lying in the same plane with the considered lattice point $l=m=n=0$; this plane again is built up by adding first the effects of points lying on a straight line going through the origin, $l=\pm1,\pm2,\ldots.\ m=n=0$

$$-\frac{p}{a^3}2\sum_1^\infty\frac{1}{l^3}.$$

Then adding the effect of subsequent straight rows, each given by $-\infty<l<\infty$, m any value $\pm1,\pm2,\pm3\ldots$ This gives

$$-\frac{p}{a}\left(4\sum_1^\infty\frac{1}{m^2}-16\pi K_1(2\pi)-40\pi K_1(4\pi)\cdots\right) \tag{4}$$

where $K_1(x)$ is connected with the "Hankel-Function" of the second kind, order 1.

Evaluating the numerical value of the effect of the zero plane gives

$$-\frac{4\pi p}{a^3}0.71 \tag{5}$$

or a little less than the total value

$$-\frac{4\pi p}{a^3}\cdot\frac{2}{3} \tag{6}$$

If instead of the "structured plane" we had a uniform plane with a "surface polarization" of p/a^2 for 1 cm^2 and a circular hole of radius a, the field in the center of the hole would be

$$-\frac{4\pi p}{a^3}\cdot\frac{1}{2}$$

We can write Equation 5

$$-\frac{4\pi p}{a^3}+\frac{4\pi}{a^3}p\cdot0.29 \tag{7}$$

the first member reducing the electric displacement to the electric force, the second member being the Lorentz-Lorenz force due to the zero plane.

The next planes below and above, $n=\pm 1$, add to this latter

$$\frac{4\pi p}{a^3}\cdot 8\pi\left[(2)^{1/2}e^{-2\pi(2)^{1/2}}+2(5)^{1/2}e^{-2\pi(5)^{1/2}}+\cdots+e^{-2\pi}+2e^{-4\pi}\right]=\frac{4\pi p}{a^3}0.052 \quad (8)$$

while the following planes $n=\pm 2$ contribute the negligible amount.

$$\frac{4\pi p}{a^3}8\pi\left[(2)^{1/2}e^{-4\pi(2)^{1/2}}+\cdots e^{-4\pi}+\cdots\right]=\frac{4\pi p}{a^3}\cdot 88\cdot 10^{-4}$$

This means that the planes $|n|>1$ are so distant, that their structure can be neglected, a uniform double layer of "surface momentum" p/a^2 giving no effect outside the layer. Concluding, we see, that the main effect of the dielectric (first member in 7) and the principal part of the Lorentz-Lorenz force is due to the zero plane, the plane ± 1 contributing slightly to the latter part.

(c) *Tetragonal lattice.* If we subject the crystal to a uniform strain along an axis, the lattice will take a tetragonal symmetry. The lattice distance in two of the axes will be a (different from the value in the unstrained crystal, which we shall call from now on a_0), along the axis of the strain it will be b. We introduce

$$\delta=\frac{b-a}{a}$$

and assume δ small in comparison with one.

We have then to distinguish two cases.

(α) strain parallel to the electric force.

Lattice points at $x=la$, $y=ma$, $z=nb=na(1+\delta)$

In calculating the force on one dipole, the effect of the zero plane is again given by 4, 5, 7, if only we substitute everywhere the present value of a. The influence of the planes $n=\pm 1$ is modified (lessened for $\delta>0$), because the distance is changed. Instead of (8) we get

$$\frac{4\pi p}{a^3}\cdot 8\pi\left[(2)^{1/2}e^{-2\pi(2)^{1/2}}(1-2\pi(2)^{1/2}\delta)+2(5)^{1/2}e^{-2\pi(5)^{1/2}}(1-2\pi(5)^{1/2}\delta)\cdots\right.$$
$$\left.+e^{-2\pi}(1-2\pi\delta)+2e^{-4\pi}(1-4\pi\delta)+\cdots\right]$$

The end result is therefore

$$-\frac{4\pi p}{a^3}\left[\frac{2}{3}+16\pi^2\delta(2e^{-2\pi(2)^{1/2}}+10e^{-2\pi(5)^{1/2}}+\cdots+e^{-2\pi}+6e^{-4\pi}+\cdots)\right]$$
$$=-\frac{4\pi p}{a^3}\left[\frac{2}{3}+0.343\delta\right] \quad (9)$$

(β) In the case of a strain at right angles to the electric field, f.e. parallel y, we have $x=la$; $y=mb=ma(1+\delta)$; $z=na$

Here the formulas are a little more complicated, because the effect of the zero plane is also modified. Developing Madelung's formula by powers of δ, we find for the zero-plane

$$-\frac{4\pi p}{a^3}\left[.71-2\pi\delta\left(\frac{1}{\pi^2}\sum_1^\infty\frac{1}{m^2}+4K_1'(2\pi)+20K_1'(4\pi)\cdots\right)\right]$$

The following planes give

$$\frac{4\pi p}{a^3}8\pi(1-\delta)\left[(2)^{1/2}e^{-2\pi(2)^{1/2}}\left(1-\frac{\delta}{2}+\frac{2\pi}{(2)^{1/2}}\delta\right)+2(5)^{1/2}e^{-2\pi(5)^{1/2}}\left(1-\frac{\delta}{2}+\frac{2\pi}{2}(5)^{1/2}\delta\right)\cdots+e^{-2\pi}\left(1-\frac{\delta}{2}+\pi\delta\right)+3e^{-4\pi}\left(1-\frac{\delta}{2}+2\pi\delta\right)+\cdots\right]$$

The end result is

$$-\frac{4\pi p}{a^3}\left(\frac{2}{3}-1.168\delta\cdot\right) \tag{10}$$

It would follow then

$$-\frac{2n(n_1-n_\perp)}{(n^2-1)^2}=(0.341+1.168)\delta$$

Ewald has calculated the left hand expression with his method for $\delta=-0.107$ and found 0.179, while our formula would give 0.161. The difference can be explained by the fact that for such a large δ higher powers have to be considered.

(d) *Rocksalt lattice.* If we consider a particle A at the origin and call now a the distance to the next particle of the same kind, the lattice of rocksalt is constituted by 8 elementary lattices, the origins of which are given by

	I	$x=0$	$y=0$	$z=0$	V	$x=0$	$y=\frac{a}{2}$	$z=0$
A	II	$\frac{a}{2}$	$\frac{a}{2}$	0	B VI	$\frac{a}{2}$	0	0
	III	0	$\frac{a}{2}$	$\frac{a}{2}$	VII	0	0	$\frac{a}{2}$
	IV	$\frac{a}{2}$	0	$\frac{a}{2}$	VIII	$\frac{a}{2}$	$\frac{a}{2}$	$\frac{a}{2}$

Calculation shows that lattice I gives the factor $-2/3$ while the others do not give simple numbers when taken separately; but II+III+IV give $-3.2/3$, while V+VI+VII+VIII give $-4.2/3$.

But it is not necessary to carry the calculations (except 000) through for all lattices. It is simpler first to assume all lattice points occupied by particles B, which would give a simple latice I. Then we substitute in the first four lattices A for B or add A-B. Written symbolically, the roman numbers now standing for the numerical coefficient (bracket expressions like the one in Equation 9) we get the force of the polarization on a particle A

$$-\frac{4\pi p_B}{a^3}8I-\frac{4\pi}{a^3}(p_A-p_B)(\mathrm{I}+\mathrm{II}+\mathrm{III}+\mathrm{IV}) \tag{11}$$

The details of the calculations can be found in the appendix. The resulting effect on a particle A is

(a) for stress parallel to the electric force

$$-\frac{4\pi}{a^3}p_A 4\left(\frac{2}{3}-0.585\delta\right)-\frac{4\pi}{a^3}p_B 4\left(\frac{2}{3}+1.248\delta\right) \tag{12a}$$

(b) for stress at right angles to the electric force.

$$-\frac{4\pi}{a^3}p_A 4\left(\frac{2}{3}-0.081\delta\right)-\frac{4\pi}{a^3}p_B 4\left(\frac{2}{3}-2.255\delta\right) \tag{12b}$$

3. THE CHANGES IN REFRACTIVE INDEX

If we write equations (12) in general

$$-\frac{4\pi}{a^3}p_A 4\left(\frac{2}{3}+\alpha\delta\right)-\frac{4\pi}{\alpha^3}p_B 4\left(\frac{2}{3}+\beta\delta\right)$$

we can now use the following formulas, if we assume that r_A, r_B take the values $r_A(1+\gamma_A\delta)$, $r_B(1+\gamma_B\delta)$

$$\frac{4\pi}{3}p_A=r_A(1+\gamma_a\delta)\left[D-\frac{4\pi}{a^3}p_A 4\left(\frac{2}{3}+\alpha\delta\right)-\frac{4\pi}{a^3}p_B 4\left(\frac{2}{3}+\beta\delta\right)\right] \tag{13}$$

and a corresponding equation for B. We divide through by a^3, defined according to equation (3)

$$4\frac{4\pi}{a^2 b}p_A+4\frac{4\pi}{a^2 b}p_B=\frac{n^2-1}{n^2}D$$

and introduce

$$4\frac{r_A}{a_0{}^3}=R_A \quad 4\frac{r_B}{a_0{}^3}=R_B \quad \text{so that } R_A+R_B=\frac{n_0{}^2-1}{n_0{}^2+2}$$

Finally, we write

$$a=a_0(1+\delta') \text{ and } \epsilon=\frac{R_A}{R_B}$$

The solution of equation (13) is, if we keep only the first power in δ and δ'

$$\Delta n = \frac{n_0^2-1}{2n_0}\left\{\delta\left(\frac{n_0^2+2}{3}\,\frac{\epsilon\gamma_A+\gamma_B}{1+\epsilon}-n_0^2\right)-\delta'(n_0^2+2)\right\}$$
$$-\frac{(n_0^2-1)^2}{2n_0}\delta\left[\alpha+\frac{2\epsilon}{(1+\epsilon)^2}(\beta-\alpha)\right] \qquad (14)$$

We have now to write down this equation separately for the two cases mentioned in 12a and b, using each time the right values of α and β, and then subtract.

If the index e indicates electric force parallel to the direction of compression (optical axis, extraordinary ray) and o electrical force at right angles (ordinary ray), we get

$$n_e-n_0=\frac{(n^2-1)^2}{2n}\left[\frac{1}{3}\,\frac{n^2+2}{n^2-1}\,\frac{\epsilon(\gamma_{Ae}-\gamma_{A0})+\gamma_{Be}-\gamma_{B0}}{1+\epsilon}\right.$$
$$\left.+\left(0.504-\frac{2\epsilon}{(1+\epsilon)^2}4.007\right)\right]\delta \qquad (15)$$

Probably the coefficients are 0.5 and 4.

4. THE ELASTIC DEFORMATIONS

The elastic relations in a crystal of the rocksalt type pressed uniformly with the pressure $P\|z$ can be written

$$0=X_x=c_{11}x_x+c_{12}y_y+c_{12}z_z$$
$$0=Y_y=c_{12}x_x+c_{11}y_y+c_{12}z_z$$
$$-P=Z_z=c_{12}x_x+c_{12}y_y+c_{11}z_z$$

This leads to

$$x_x=y_y=\delta'=+\frac{c_{12}}{c_{11}^2+c_{11}c_{12}-2c_{12}^2}P$$
$$z_z=\delta'+\delta=-\frac{c_{11}+c_{12}}{c_{11}^2+c_{11}c_{12}-2c_{12}^2}P$$
$$\delta=-\frac{c_{11}+2c_{12}}{c_{11}^2+c_{11}c_{12}-2c_{12}^2}P=-\frac{P}{c_{11}-c_{12}}$$

According to the measurements of Voigt[12] and Forsterling,[13] we get for $P=\dfrac{1\text{ kg}}{\text{cm}^2}$

$$\text{NaCl } \delta=-2{,}9\cdot 10^{-6} \quad \text{KCl } \delta=-3{,}13\cdot 10^{-6}$$

[12] W. Voigt, Gott. Nachr., p. 330; 1880.
[13] K. Forsterling, ZS. f. Phys., *2*, p. 172; 1920.

5. THE RESULTS

ϵ was calculated from the formulas of Herzfeld and Wolf.[14]

Mr. Maris measures directly the retardation in multiples of the wave length for 1 cm length, but we will give instead of it the differences in the refractive index themselves because these turn out to vary much less with the wave length.

$10^7\ (n_e - n_o)$ for 1 kilogram per 1 cm^3

λ	NaCl			KCl		
	Calc.	Exp.	Exp. / Calc.	Calc.	Exp.	Exp. / Calc.
4359	1.382	2.197 M	1.59	−12.98	−2.973 M	0.228
5461	1.185	2.059 M	1.74	−12.67	−2.900 M	0.228
5790	1.152	1.922 M	1.62	−12.56	−2.895 M	0.230
5890	—	2.200 P	—	—	−2.78 P	—

M means Maris; P Pockels.

The difference in sign for NaCl and KCl is due to the fact that in NaCl the molrefraction of Na is very small in comparison with the one of Cl, and therefore the whole effect is due to the action of Cl ions on other Cl ions while in potassium chloride we have a much larger molrefraction of the K, and therefore the action of opposite ions (K and Cl) on each other has to be taken into account. Now on account of the geometrical distribution this action has the opposite sign.

6. THE ABSOLUTE CHANGES IN REFRACTIVE INDEX

Pockels has measured also the absolute retardations from which the absolute changes in refractive index can easily be found. One finds from his data 2.67×10^{-7} and 4.87×10^{-7}. Now our formula would give, if we put the γ zero, approximately 14.2×10^{-7} and 15.4×10^{-7}. Therefore there must be a strong change in the molrefraction of the ions under the influence of stress in both directions (parallel and at right angles to the stress) to bring the results into agreement. If one would ascribe the whole change in NaCl to the Cl ion and then apply the γ which are calculated from this, to the case of KCl neglecting any change in the K ions, the change in the calculated values would only

[14] K. F. Herzfeld and K. L. Wolf, Ann. d. Phys., *78*, p. 35; 1925.

amount to a few percent and therefore would be far too small to account for the disagreement.

7. CONCLUSIONS

The double refraction in crystals of rocksalt and sylvine under stress can be not be explained wholly by assuming the effect to be due only to the Lorentz-Lorenz force.

PHYSICS DEPARTMENT,
JOHNS HOPKINS UNIVERSITY,
BALTIMORE, MARYLAND.
APRIL, 1928.

MATHEMATICAL APPENDIX

Stress parallel z, electrical force $\| z$.

Lattice I is given in the text.

Lattice II: zero plane, $x=\frac{a}{2}+la,\ y=\frac{a}{2}+am$

$$\frac{32\pi p}{a^3}[-K_1(\pi)+2K_1(2\pi)-(3+1)K_1(3\pi)+\cdots]-\frac{16p}{a^3}\sum_1\frac{1}{(2m+1)^2}$$

Next planes $z=\pm a(1+\delta)$

$$\frac{32\pi^2 p}{a^3}[(2)^{1/2}e^{-2\pi(2)^{\frac{1}{2}}}(1-2\pi(2)^{1/2}\delta)-2(5)^{1/2}e^{-2\pi(5)^{\frac{1}{2}}}(1-2\pi(5)^{1/2}\delta)+\cdots$$
$$-e^{-2\pi}(1-2\pi\delta)+2e^{-4\pi}(1-4\pi\delta)\cdots]$$

over next planes $z=\pm 2a(1+\delta)$

$$\frac{32\pi^2 p}{a^3}[(2)^{1/2}e^{-4\pi(2)^{\frac{1}{2}}}(1-4\pi(2)^{1/2}\delta)\cdots-e^{-4\pi}(1-4\pi\delta)\cdots]$$

Lattice III and IV. $x=la,\ y=\frac{a}{2}+ma$ and $x=\frac{a}{2}+la,\ y=ma$

Two closest planes, $z=\pm\frac{a}{2}(1+\delta)$

$$\frac{64\pi^2 p}{a^3}[-(2)^{1/2}e^{-\pi(2)^{\frac{1}{2}}}(1-\pi(2)^{1/2}\delta)+2(2)^{1/2}e^{-2\pi(2)^{\frac{1}{2}}}(1-2\pi(2)^{1/2}\delta)$$
$$-2(10)^{1/2}e^{-\pi(10)^{\frac{1}{2}}}(1-\pi(10)^{1/2}\delta)\cdots+2e^{-2\pi}(1-2\pi\delta)+\cdots]$$

Next planes $z=\pm\frac{3}{e}a(1+\delta)$

$$\frac{64\pi^2 p}{a^3}[-(2)^{1/2}e^{-3\pi(2)^{\frac{1}{2}}}(1-3\pi(2)^{1/2}\delta)+\cdots]$$

Stress parallel x, electric force $\| z$.
Lattice I is given in the text.
Lattice II,

$$x=(\tfrac{1}{2}+l)a(1+\delta) \qquad y=(\tfrac{1}{2}+m)a$$

Zero plane:

$$\frac{32\pi^2 p}{a^3}(1-\delta)\left[-K_1(\pi)-K_1'(\pi)\pi\delta+2K_1(2\pi)+2K_1'(2\pi)2\pi\delta-K_1(3\pi)\right.$$
$$\left.-4K_1'(3\pi)3\pi\delta\right]-\frac{16p}{a^3}(1-2\delta)\sum\frac{1}{(2m+1)^2}$$

next planes $z=\pm a$

$$\frac{32\pi^2 p}{a^3}(1-\delta)\left[(2)^{1/2}e^{-4\pi(2)^{\frac{1}{2}}}\left(1-\frac{\delta}{2}+\frac{2\pi}{2}(2)^{1/2}\delta\right)-2(5)^{1/2}e^{-2\pi(5)^{\frac{1}{2}}}\right.$$
$$\left.\left(1-\frac{\delta}{2}+\frac{2\pi}{2}(5)^{1/2}\delta\right)+\cdots-e^{-2\pi}\left(1-\frac{\delta}{2}+\pi\delta\right)\cdots\right]$$

Lattices III and IV.

III $x=(\tfrac{1}{2}+l)a(1+\delta),\ y=ma$ IV $x=la(1+\delta),\ y=(\tfrac{1}{2}+m)a$

Closest planes $z=\pm\dfrac{a}{2}$

$$\frac{64\pi^2 p}{a^3}(1-\delta)\left[-(2)^{1/2}e^{-\pi(2)^{\frac{1}{2}}}\left(1-\frac{\delta}{2}+\frac{\pi}{2}(2)^{1/2}\delta\right)+2(2)^{1/2}e^{-2\pi(2)^{\frac{1}{2}}}\right.$$
$$\left(1-\frac{\delta}{2}+\pi(2)^{1/2}\delta\right)+\cdots+2e^{-2\pi}\left(1-\frac{\delta}{2}+2\pi\delta\right)$$
$$\left.+2e^{-4\pi}\left(1-\frac{\delta}{2}+4\pi\delta\right)\cdots\right]$$

next planes, $z=\pm\dfrac{3}{2}a$

$$\frac{64\pi^2 p}{a^3}(1-\delta)\left[-(2)^{1/2}e^{-3\pi(2)^{\frac{1}{2}}}\delta\left(1-\frac{\delta}{2}+\frac{3\pi(2)^{1/2}}{2}\delta\right)+\cdots\right]$$

TEMPERATURE OF THE UNDER-WATER SPARK AS COMPUTED FROM DISTRIBUTION OF INTENSITY IN OH ABSORPTION BANDS

By Earl D. Wilson

ABSTRACT

Detailed measurements of the OH-bands found absorbed in the under-water spark reveal that the system is developed in absorption almost as completely as in emission. Calculations based on intensity distribution lead to a value of approximately 5000°C for the effective temperature of the source.

INTRODUCTION

The strong "water band" at λ3064, now ascribed to the carrier OH, was discovered in emission in 1880. Credit for the discovery is shared in the literature between Huggins[1] and the pair of investigators Liveing and Dewar,[2] who later examined the whole band system in the ultraviolet. The accurate and extensive measurements of wave lengths for the band at λ3064 made in 1912 by Grebe and Holtz,[3] were used by Heurlinger[4] in 1918 for quantum analysis. Heurlinger succeeded in arranging almost all of Grebe and Holtz's lines into twelve parabolic series, forming two distinct bands of three double branches each. The stronger band headed at λ3064, while the weaker headed at λ3126 (less refrangible R-branch).

Six years later Watson[5] measured and analyzed in an exactly similar manner the band λ2811 together with its weaker neighbor at λ2875. Finally in 1927 Jack[6] measured and classified the lines of the band at λ2608. The additional experimental and theoretical work of other investigators leave little to be desired with respect to the analysis of the band system in emission, and altogether make it quite probable that the carrier is OH.

That the OH-bands occur also in absorption under various conditions is very well known. We may refer to the work of Deslandres,[7] of Liveing and Dewar,[8] and of Fowler[9] on the presence of "water

[1] Huggins, Proc. Roy. Soc., *30*, p. 576; 1880.
[2] Liveing and Dewar, Proc. Roy. Soc., *30*, p. 494; 1880.
[3] Grebe and Holtz, Ann. d. Phys., *39*, p. 1243; 1912.
[4] Heurlinger, Dissertation, Lund, 1918.
[5] Watson, Astrophys. Journ., *60*, p. 145; 1924.
[6] Jack, Proc. Roy. Soc., *115*, p. 373; 1927.
[7] Deslandres, Comptes Rendus, *100*, p. 854; 1885.
[8] Liveing and Dewar, Phil. Trans., *179*, p. 27; 1888.
[9] Fowler, Proc. Roy. Soc., *94*, p. 472; 1917–18.

bands" in absorption in the solar spectrum; or to the work of Hulthen and Zumstein[10] on the ready absorption of the band at λ3064 by the oxyhydrogen flame. More than twenty-five years ago Konen[11] mentioned the reversal of the "water bands" in the under-water spark; and during the last quarter of a century many investigators who have employed the under-water spark as a source of continuous radiation in the ultraviolet have reported more or less incidentally the presence of these bands in absorption in the source.

It has been the purpose of the writer, first, to measure all the lines appearing in the under-water source in order to ascertain how fully the bands are developed in such absorption; and, secondly, to measure in so far as possible the intensities of the lines in the various branches. Since Birge[12] has been successful in relating the distribution of intensity in band spectra to the temperature of the source in a rather simple manner, it is hoped that it might be possible to compute from such measurements of intensity the effective temperature of the under-water spark.

SPECTROGRAPHIC PROCEDURE

The electrical circuit employed to produce the under-water spark is outlined in Fig. 1. The energy was supplied from 110-volt, A.C. mains through a ballast resistance to the primary of a 2½k.v.a. trans-

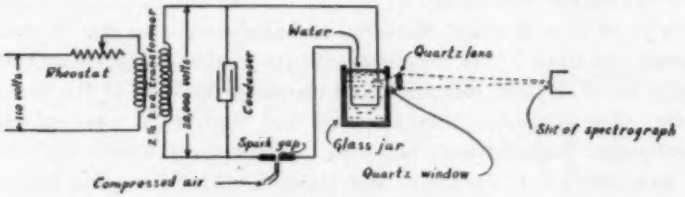

FIG. 1. *Diagram of apparatus*

former. The secondary, at a tension of 20,000 volts, charged a large condenser which in turn produced a high-frequency oscillatory discharge through an external auxiliary spark gap and an under-water gap in series. The auxiliary gap, about 1 cm in length, was quenched by means of a strong continuous blast of air. For the under-water gap aluminum electrodes, 5 mm in diameter, were employed. They were provided with wedge-shaped terminals whose edges were oriented so

[10] Hulthen and Zumstein, Phys. Rev., *28*, p. 13; 1926.
[11] Konen, Ann. d. Phys., *9*, p. 742; 1902.
[12] Birge, Astrophys. Journ., *55*, p. 273; 1922.

as to lie parallel to the axis of collimation. The distance between the terminals was of the order of 1 mm.

The medium for the spark was tap water in slow circulation. It was contained in a glass jar provided with a quartz window before which was permanently attached a small quartz condensing lens of diameter 2.5 cm, and focal length 5 cm. This single lens was so situated as to project upon the slit of the spectrograph a magnified image of the source just large enough to fill the exposed part of the slit (3mm) with ultraviolet light, and yet not large enough to dissipate the energy transferred.

The spectrograph, made by Hilger, was of the E-1 type, having a dispersion of about 5.3A per mm at λ3064 and about 3.9A per mm at λ2811. It was focused for the region from λ2600 to λ4000. The slit width was adjusted to 3 divisions from the actual zero.

Since the absorbing medium lay in the source itself, the taking of the pictures was comparatively simple. In accordance with the usual practice, the spectrum of an iron arc was photographed above and below each spectrum from the under-water source. Length of exposures for the latter ranged from 1 sec. to 10 min. The plates selected for measurement were simply those which under microscopic examination revealed the sharpest structure for the OH-bands.

PHOTOMETRIC PROCEDURE

No direct measurements of wave length were made from the plates, but from intensity curves traced by a Moll microphotometer. To secure photometer records from which measurements both of wave lengths and intensities could be made, a select plate was adjusted in the instrument so that the band structure would traverse the incident beam, and the trace was completed in the usual manner. Then the instrument being returned to its initial position, a trace for the comparison emission spectrum of iron was registered on the same strip of sensitized paper. The result was that the systems of absorption and emission lines extended toward each other, frequently being quite adjacent at their peaks.

MEASUREMENTS OF WAVE LENGTHS

A special form of comparator fitted with a low-power objective was employed to measure the wave lengths of the absorption lines directly from the photometric prints by comparison with the iron lines. A graphical method of interpolation reduced scalar readings to Angstrom

units and automatically corrected for prismatic curvature on the plate and the possible lateral displacement of the plate during the photometric process.

DESCRIPTION OF RESULTS

The measurements revealed the presence of all the double branches in Watson's bands at λ2811 and λ2875 as well as all the double branches in Heurlinger's bands at λ3064 and λ3126.

By comparison with Watson's data (employing conventional notation) all the members of the R_1 branch of band λ2811 from $m=2$ to $m=19$, inclusive, were identified, only members 5 and 12 being doubtful. Also in the R_2 branch, members from quantum number 2 to number 19 were all found. In the Q_1 branch, lines 2 to 22 were all identified but number 23 could not be located. The Q_2 branch contained every one of the lines from $m=2$ to $m=22$, a twenty-third line not being listed in emission. Of the lines in the P_1 branch, those from $m=2$ to $m=21$ were identified, the twenty-second not being found. The presence of members 4 and 21 was rather doubtful. Similarly, in the P_2 branch, lines 2 to 21 were found, the twenty-first being doubtful and the twenty-second not being located.

In the weaker band at λ2875, the R_1 branch yielded lines $m=5, 6, 8$ out of Watson's 4 to 8 inclusive, number 5 being doubtful, and 6 and 8 coincident; but the R_2 branch contained all the listed members 4 to 8. In each of the branches Q_1 and Q_2 all the lines from $m=2$ to $m=11$ were identified. In the P_1 branch, member 5 was doubtful, while all the remaining ones from 2 to 12 were definitely located. The P_2 branch yielded all the listed lines from 2 to 11, but lines 3 and 6 were uncertain.

Now for these two bands in the spectral region of shorter wave lengths, the dispersion was happily adequate to a practically complete separation of lines. However, in Heurlinger's bands at λ3064 and λ3126, the dispersion was less, and consequently lines were sometimes unresolved, making the identification more difficult.

In the strong band at λ3064, out of Heurlinger's listed lines $m=2$ to $m=25$ for the R_1 branch, seventeen were identified. Numbers 2, 19, 20 and 22 were concealed by two strong aluminum absorption lines. Numbers 6, 7, and 11 were too near stronger lines to be resolved. We add also that the measurements of lines 10, 12, 13, 23 and 25 (as in the case of certain other lines in this band) were somewhat inaccurate because of lack of resolution. In the R_2 branch, lines 4 to 22 were found, but numbers 2, 3, 10 and 21 were unresolved, and number 20 was hidden

by an aluminum line. The Q_1 branch contained the listed lines from $m=2$ to $m=29$, except that number 26 was not found, and lines 14, 17 and 29 were doubtful. In the Q_2 branch, aside from four concealed lines, all members were identified except the last three, and line 15 was uncertain. In the P_1 and P_2 branches, which ran out to the longest wave lengths, lines 24 to 28 could not be definitely located because of faintness. In the latter branch also line 8 was not found.

For the weaker band at λ3126 (head of R_1 branch), lines 5, 7, 8 and 9 were not found in the listed lines from $m=5$ to $m=14$ in the R_1 branch. Of the eight lines (at least) belonging to the R_2 branch, which Heurlinger did not analyze, six were identified from Grebe and Holtz's measurements. In the Q_1 branch, all the lines were found from $m=3$ to $m=20$ except numbers 5, 12, 13, 16, 19, and 20. Out of t he 19 listed lines for the Q_2 branch, only lines 2, 6, and 14 could not be found. The P_1 branch yielded nine lines out of fifteen, but again in the P_2 branch all members were identified from $m=2$ to $m=17$ as listed except numbers 5, 7 and 13. Also lines 16 and 17 were uncertain.

As a summary of the results of the line measurements, the following statements may be clarifying. Watson records 121 lines for the band at λ2811. Of these lines 113 have been identified with possibly 5 more lines doubtful. For the weak band at λ2875 Watson measured 51 lines. Of this band 45 lines have been found in absorption, with possible addition of 4 doubtful ones. For the band at λ3064, of the 145 lines classified by Heurlinger which lay within the range of wave lengths contained on the print, 139 were either directly identified or accounted for in unresolved lines, with 3 additional doubtful ones. In the weak band at λ3126 (head of the R_1 branch there were found 64 of the 76 lines listed by Heurlinger, with possibly 2 more. Of the total 247 lines in both bands measured by Grebe and Holtz in the range investigated in this paper, 222 were identified, 3 more being doubtful. It is interesting to note that several of the lines either not accounted for or not found at all on the prints are not tabulated in Heurlinger's classification of the branches, but are included in the complete tables of Grebe and Holtz.

As an illustration of the completeness of development of the branches in absorption, and to gauge the order of accuracy involved in the measurements, we append the following table for the Q branches of Watson's band at λ2811.

In these forty-two measurements, the largest single deviation from

TABLE 1. *Comparison of lines measured in absorption with those measured in emission band at λ2811*

Branch Q_1				Branch Q_2			
m	λ (I. A.) Watson	λ (I. A.) Writer	Δλ	m	λ (I. A.) Watson	λ (I. A.) Writer	Δλ
2	2829.25	2829.23	−0.02	2	2819.13	2819.19	+0.06
3	28.95	28.93	− .02	3	20.66	20.64	− .02
4	29.35	29.34	− .01	4	22.39	22.44	+ .05
5	30.31	30.28	− .03	5	24.37	24.43	+ .06
6	31.81	31.80	− .01	6	26.65	26.62	− .03
7	33.82	33.77	− .04	7	29.25	29.23	− .02
8	36.30	36.32	+ .02	8	32.20	32.17	− .03
9	39.21	39.21	.00	9	35.51	35.49	− .02
10	42.62	42.60	− .02	10	39.21	39.21	.00
11	46.45	46.41	− .04	11	43.27	43.22	− .05
12	50.72	50.71	− .01	12	47.75	47.78	+ .03
13	55.43	55.42	− .01	13	52.65	52.67	+ .02
14	60.60	60.59	− .01	14	57.96	57.93	− .03
15	66.23	66.30	+ .07	15	63.71	63.70	− .01
16	72.32	72.26	− .06	16	69.90	69.91	+ .01
17	78.87	78.86	− .01	17	76.55	76.54	− .01
18	85.91	85.92	+ .01	18	83.69	83.70	+ .01
19	93.47	93.44	− .03	19	91.29	91.31	+ .02
20	2901.54	2901.48	− .06	20	99.42	99.42	.00
21	10.05	10.02	− .03	21	2907.99	2908.04	+ .05
22	19.18	19.20	+ .02	22	16.92	17.00	+ .08
23	28.88						

Watson's values is 0.08 Angstrom, and this difference is for a very faint line. The average of the absolute values of Δλ is 0.03. This value may fairly be taken as the order of accuracy to be expected in the measurements described.

MEASUREMENTS OF INTENSITY

The law of photographic blackening together with the empirical results of G. R. Harrison[12] on the characteristics of panchromatic emulsions leads rather directly to a simple approximation formula for the intensity of weak lines in absorption, namely

$$I = k\frac{a}{d^2},$$

where a is the small area enlosed by an absorption peak on the photometer print, d is the total displacement from zero of the galvanometer

[12] G. R. Harrison, J.O.S.A. & R.S.I., *11*, p. 341; 1925.

trace on the print for the given peak, and k is a constant of proportionality. The specification of the area enclosed by the peak naturally implies that each line whose intensity is to be measured is distinct from other lines so that there is no overlapping of areas. Unfortunately, this restriction is not generally satisfied in the OH-bands under experimental conditions. Although the band at λ2811 most nearly approaches complete separation of lines, its faintness made the value of a too small to be measured with any certainty. The strongest band at λ3064 provided measureable values of a, but the dispersion, was not quite adequate to a generally complete separation of lines. By comparing the observed wave lengths of all the peaks on the photometric print belonging to this band with Heurlinger's classification, and checking off those peaks which represented either actual coincidences or unresolved groups, it was discovered that the P_2 branch alone possessed a sufficient mumber of "free" (or nearly "free") lines to determine an intensity curve. The Q_1 branch afforded a less satisfactory set of six lines, while the P_1 branch afforded only four scattered lines. Table 2 gives the computed values of I in arbitrary units.

TABLE 2. *Intensities of certain absorption lines in the band at λ3064*

Branch P_1			Branch P_2			Branch Q_1		
m	I	λ (I. A.)	m	I	λ (I. A.)	m	I	λ (I. A.)
3	95	3096.34	5	129	3096.12	8	180	3094.61
12	128	3140.72	6	151	3101.22	12	346	3105.65
15	53	61.88	10	257	24.92	13	287	09.32
17	54	77.67	11	249	30.24	18	125	33.20
			12	200	36.87	19	66	39.14
			13	133	43.77	25	16	83.91
			14	100	50.98			
			16	67	66.32			
			18	51	82.95			
			20	31	3200.94			

THEORETICAL INTERPRETATION

Birge[14] reports that for simple types of band spectra the intensity in each branch is distributed in such a way as to satisfy the empirical relation

$$\text{intensity} = me^{-a\,m^2}$$

where m is the whole rotational quantum number for a given line and a is a parameter evidently depending on J, the moment of inertia, and

[14] Birge, Molecular Spectra in Gases, p. 155; 1927.

on T, the absolute temperature. This empirical relation is the same as that deduced by Kemble[15] from classical theory. By inserting the expression

$$E_m = \frac{m^2 h^2}{8\pi^2 J}$$

for the energy of rotation into Maxwell's distribution function and combining with the above equation, there results

$$\text{Intensity} = cme^{-m^2h^2/8\pi^2JkT}$$

By differentiating with respect to m and equating to zero,

$$m_{\max} = \frac{2\pi}{h}(kJT)^{1/2}$$

or,

$$T = \frac{h^2}{4\pi^2 kJ} \cdot m_{\max^2},$$

which states that the effective temperature of the source is, for a given type of molecule, determined by the whole rotational quantum number of the line in a branch which has maximum intensity. Recalling that h is Planck's constant (6.55×10^{-27}) and k is the molecular gas constant (13.72×10^{-17}), our equation reduces to

$$T = 79.2\times10^{-40}\frac{m_{\max^2}}{J}.$$

Fig. 2 is a graphical representation of the central columns of Table 2, the intensity being plotted against corresponding quantum numbers of the P_2 branch. There is no doubt that a maximum exists in the neighborhood of $m=10$, and is apparently at about $m=10.2$. The data for the other two branches, although not decisive, are of such a nature as to corroborate this result.

There remains yet the value of J to be inserted into the formula. In the theory this moment of inertia is assumed to be constant during an absorption process. Birge's[16] tables give for the initial J in emission for the OH carrier with respect to the band at λ3064,

$$J' = 1.63\times10^{-40}$$

[15] Kemble, Phys. Rev., *8*, p. 689; 1916.

[16] Birge, Molecular Spectra in Gases, p. 232; 1927.

and for the final J in emission

$$J''=1.43\times10^{-40}.$$

Hence we take the average value, $J=1.53\times10^{-40}$ for our computations. Thus

$$T=\frac{79.2\times10^{-40}}{1.53\times10^{-40}}\cdot(10.2)^2$$

$$=5387^\circ \text{ Abs.}$$

$$=5115^\circ C, \text{ approximately}$$

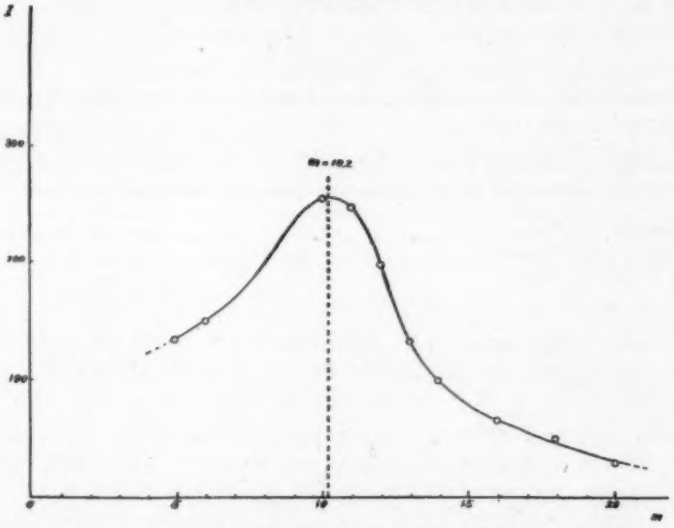

FIG. 2. *Curve showing intensities of lines in P_2 branch of band at λ3064.*

It is not unreasonable to expect a very high temperature in the under-water spark, when one considers the spectroscopic data. The OH-bands have the assigned vibrational quantum numbers as follows: λ3064 = 0, 0; λ3126 = 1, 1; λ2811 = 1, 0; λ2875 = 2, 1. Under ordinary conditions of absorption one should expect to find only those bands which correspond to transitions of vibrational energy from the normal vibrationless state ($n''=0$) to higher quantum states. This would produce the strong band λ3064 (0, 0) and the weaker band λ2811 (1, 0). The fact that our data show that also bands λ3126 (1, 1) and λ2875 (2, 1) occur, certainly indicates that the temperature of the carrier OH in the source was great enough to cause an appreciable fraction of them to be in the first vibrational quantum state.

SUMMARY

1. Measurement of the wave lengths of lines observed in the OH-bands absorbed in the under-water sparks shows that the bands at λ2811, λ2875, λ3064 and λ3126 are developed almost as fully as in emission.

2. Measurement of intensity in branches of the bands at λ3064 reveals a maximum at about $m=10.2$, from which value the effective temperature of the under-water spark has been computed from Birge's formula to be 5115°C under the existing experimental conditions.

3. Since the data indicate that a rather high temperature is to be expected in the under-water spark, the results may be considered as an empirical check upon the validity of the formula.

The writer wishes to express his indebtedness to Professor Raymond T. Birge of the University of California for assistance in calculating the effective temperature of the spark and to Professor Alpheus W. Smith who suggested the problem and gave valuable aid in the solution.

MENDENHALL LABORATORY,
OHIO STATE UNIVERSITY,
COLUMBUS, OHIO.

INSTRUMENT SECTION

AN IMPROVED PERMEAMETER FOR TESTING MAGNET STEEL

By B. J. Babbitt

INTRODUCTION

The increasing use of cobalt steel in the manufacture of permanent magnets has created a need for a permeameter that is capable of determining accurately the magnetic properties of such steel in bar form. The common commercial permeameters are not capable of producing the high magnetizing forces required for this purpose. Commercial permeameters are chiefly of two types, the yoke type and the Burrows type. The latter is difficult to operate and requires an experienced operator for a reasonable output; it cannot be adapted to the testing of cobalt steel unless it is practically rebuilt throughout. The yoke type of permeameter may be adapted to the testing of cobalt steel by the use of extensions to the poles so that the distance between them is much less. In this way the greater part of the magnetomotive force is distributed over a short portion of the magnetic circuit and the magnetomotive force per centimeter is correspondingly greater. The permeameter that is described below has been developed by the Magnetic Materials Division at the Hawthorne Works of the Western Electric Company to overcome the chief objections common to present commercial permeameters.

DESIGN AND CONSTRUCTION

A study of the characteristics desirable in a permeameter for testing magnet steel resulted in the selection of the following points as being of greatest merit in such an instrument.

1. Capability of developing uniform magnetizing forces as great as 1000 gilberts per centimeter or greater. 2. A high degree of accuracy. 3. Simplicity of set-up, combined with ease and rapidity of operation.

A study of the magnetizing field of a yoke type permeameter shows it to be much stronger at the pole faces than at a point midway between the poles, and when auxiliary pole pieces are used to intensify the magnetizing field, the condition of non-uniformity is accentuated. Inasmuch as the H-coil or the coil that is used for determining the magnetizing force H is necessarily of appreciable size, it cannot be concentrated in a very restricted space wherein the magnetizing force is uniform. Consequently, it is impossible to state definitely just what value of B or magnetic induction is associated with a given value of H, as only the averages between fairly wide limits are determined. A characteristic variation in magnetizing force along the test bar is shown by Curve A, Fig. 1, which is a plot of the H-distribution along a straight line between the two poles of a U-shaped magnetic yoke

when a magnetomotive force is applied to the central portion of the yoke.

It should be said for the yoke type of permeameter that in a great many cases the condition of non-uniformity of magnetizing force is not objectionable, and may even serve to smooth out irregularities in other factors. For routine testing where it is not essential to study the finer variations, testing under conditions described may be entirely satisfacotry. In our work on tungsten steel, we have found that satisfactory results may be obtained with the Fahy Simplex permeameter when the proper care is taken both in calibrating the galvanometer with the H-coil connected in the circuit, and in the operation of the set-up.

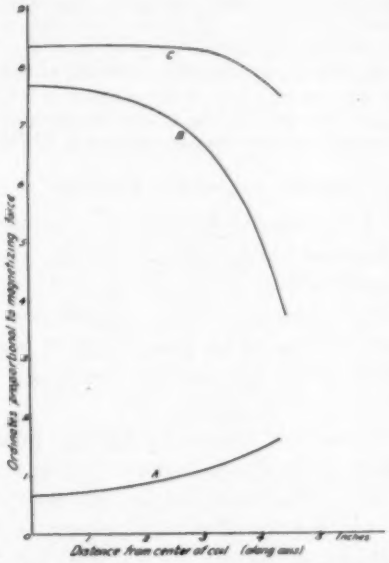

FIG. 1. *Showing variation in magnetizing forces developed by different means. A—magnetizing coil on yoke. B—short solenoid. C—A and B combined.*

It is well known that the intensity of the magnetic field produced by a solenoid drops off at the ends, being considerably greater in the central portion. This effect becomes more accentuated as the ratio of length to diameter is decreased. Such a characteristic distribution is shown by Curve *B*, Fig. 1. A comparison of Curves *A* and *B* of Fig. 1 suggested that by combining the two types of distribution a

reasonably uniform magnetic field would result. This was tried, and it was found that when the number of turns of the solenoid was about four times as great as the number of the yoke, the H-distribution inside the solenoid was very satisfactory as shown by Curve C, Fig. 1.

When it was established that a uniform magnetizing field could be obtained in this manner, the question arose as to whether saturation effects in the yoke would cause the distribution of magnetizing force to vary as its magnitude was changed. The distribution was found to change somewhat, as discussed later, but the magnetizing field throughout the central portion was always very uniform. The next point to be established was whether the ratio of magnetizing force, H, to magnetizing current, I, in the central portion of the solenoid was constant for a sufficiently wide range of currents. Currents were used to give a range of H-values from about 20 to 1000 gilberts per centimeter, and the variation with I of the ratio of H to I was investigated. It was found to drop off somewhat at the lower values of I about as indicated by Curve A, Fig. 2, which is plotted semi-logarithmically to bring out the lower values more plainly. This decrease in the ratio at low values of I could be attributed only to variations in the permeability of the core, and an attempt was made to build up a core composed of various materials such that its effective overall permeabiltiy would be practically constant. Four materials of different magnetic characteristics were chosen and calculations made so that the overall permeability of the yoke was 5000 at four different values of H. The necessary proportions by volume were found to be as follows:

Magnetic iron	55%
45–55 permalloy	25%
78½ permalloy	10%
Silicon steel	10%

Of course, the overall permeability is not constant but varies probably from 4500 to 6500, but these variations were not discernible in the tests we have made. Curve B of Fig. 2 is a typical example of the several runs we have made to test the constancy of the ratio, H/I.

The introduction of a test bar into the permeameter causes a greater magnetic flux through the yoke for a given applied magnetizing force than when no bar is present. Assume, as an example, that a bar, 3 square centimeters in cross section, is being tested, and has an induction B of 15,000 maxwells per square centimeter at a magnetizing force H of 100 gilberts per centimeter. The reluctance drop through-

out the yoke and with 2 mil air gaps at the ends of the bar amounts to about 50 gilberts which is about 2% of the total magnetomotive force developed. Cognizance was taken of this slight redistribution of H upon the insertion of the test bar and the auxiliary winding applied to the yoke was made just a little larger than necessary for producing an exactly uniform field with no bar in place so that when a bar of medium cross section is tested the distribution is as nearly uniform as it can be made. It might be said in this connection that when coercive forces are being determined, the flux in the bar is reduced to zero and that in the yoke is extremely low. The H-distribution then takes the pattern shown in Fig. 3, Curve C, and it is found that the ratio of H to I through-

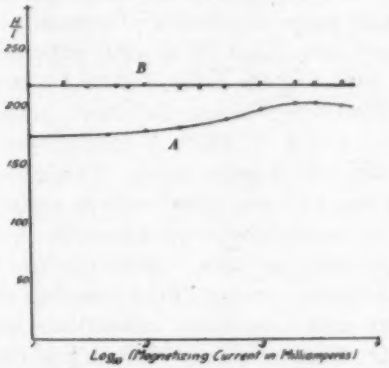

FIG. 2. *Showing variation of the ratio of magnetizing force to magnetizing current for different currents. A—first model of J-permeameter. B—present model of J-permeameter with composite yoke.*

out the central portion is the same as it is under other conditions, the difference in magnetomotive force being taken care of by the redistribution. Since the search coils extend throughout the central five-ninths of the length of the air gap, it is seen that the ratio of H to I throughout this region is constant to a high degree and that H is also sensibly uniform throughout the central portion of the test bar, the excess or lack of magnetomotive force being accommodated through slight redistribution near the poles of the yoke.

The coil used for flux determinations, or B-coil, is situated so as to cover only the portion of the test bar that is subjected to the uniform magnetizing field. When magnetizing forces as high as 200 gil/cm or so are used, the air flux in the space between the bar and the

winding of the B-coil is usually sufficient to produce an appreciable error in the indicated induction unless corrections are made to take account of it. When testing at $H=1000$ gil/cm it becomes necessary to take strict account of this additional flux. For example, assume that the area of the B-coil is 10 cm² and a bar of 1 cm² cross section is being tested, at $H_{max}=1000$ gil/cm. With a normal induction of 15,000 max/cm², corresponding to a total flux of 15,000 maxwells in the test bar, an additional flux of 9000 maxwells would thread

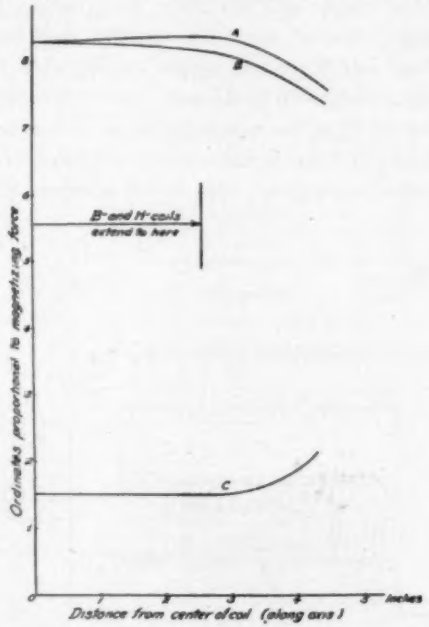

FIG. 3. *Showing slight changes in distribution of magnetizing force under different conditions. A—with no bar in permeameter. B—with large bar in permeameter. C—coercive force determination.*

through the coil due to air flux. The deflection from the B-coil would be proportional to 24,000 instead of 15,000 and a correction proportional to 9/15 of the true induction would be required. Such large corrections are detrimental to high accuracy and necessitate considerable computation. For bars of smaller cross section, such as 1/4″×1/4″, the correction due to air flux would be over half of the total deflection.

The permeameter being described, which is called the *J*- permeameter, is automatically compensated so that it records only ferric induction, which is numerically equal to $B-H$. Ordinarily this is a more expressive quantity in dealing with magnets as it is representative of the material itself. In the determination of residual induction, B_r, ferric induction only exists, and in the determination of coercive force, H_c, it makes only a very small difference whether ferric induction or total induction is reduced to zero. Ordinarily, the difference in H_c would be of the order of a few tenths of a per cent. It is believed that the art of magnetic testing is not so refined at present that such small differences are serious, but if so the proper corrections may be easily caluculated. If total induction is desired, it is only necessary to add the numerical value of H to the computed ferric induction.

The manner in which this compensation for air flux is accomplished is shown in the schematic diagram, Fig. 4. A compensating coil *C* is

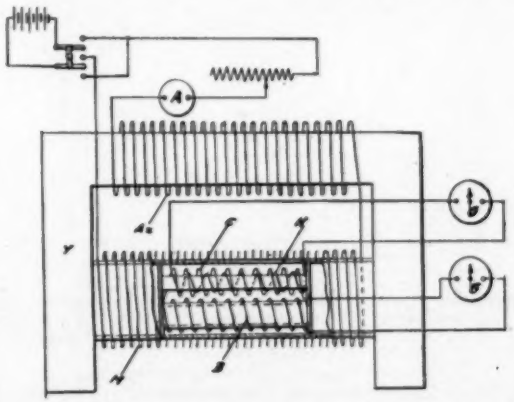

FIG. 4. *Schematic diagram showing arrangement and connections of the various windings of the J-permeameter.*

A—ammeter
A_x—auxiliary magnetizing coil
B—B-coil
C—compensating coil
G—galvanometers
H—H-coil
M—main magnetizing coil
Y—composite magnetic yoke

wound over the *H*-coil *H* and is connected in opposition to the *B*-coil *B*. Since both of these coils are always in the uniform magnetizing field, when they are so adjusted that the product AN of the number of turns by the average area of the turns of the one equals that of the other, their flux linkages will be equal and since the

coils are connected in opposition to each other, a reversal of the magnetizing field produces no deflection on an indicating galvanometer. This condition is actually obtained by individual hand adjustment and the cut-and-try method, the permeameter yoke and coil being mounted in their proper relative positions for each trial. When a good compensation is obtained at high magnetizing forces, it is found that it also holds for the lower magnetizing forces.

CALIBRATION

After it was thus established that a magnetizing field of excellent uniformity was developed, and that its value was directly proportional to the magnetizing current, it remained to establish the correct

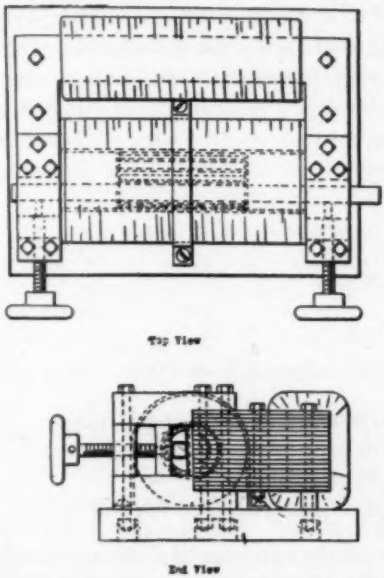

FIG. 5. *Phantom sketch showing structural details of J-permeameter.*

value of this ratio, or, in other words, to determine the absolute value of the magnetizing field. An approximate value of the magnetizing force can be determined by assuming that all of the magnetomotive force is expended over the effective length of the bar being tested. Thus

$$H=\frac{\text{m.m.f.}}{L}=\frac{.4\pi 4400I}{9.5\times 2.54}=230\ I$$

This shows that the upper limit to the ratio of H to I is about 230 gilberts per cemtimeter per ampere which is high enough to insure that it will be possible to develop the high magnetizing forces requird for testing cobalt magnet steel. The two methods of actually calibrating the instrument are described in the following paragraphs.

The first method may be called an absolute method inasmuch as it does not depend on the properties of magnetic bars previously calibrated by some accepted standard method or institution. This method employed an air-core bobbin which was placed in the uniform portion of the magnetizing field of the permeameter in such a manner that a reversal of the field produced a deflection of a galvanometer connected to the bobbin. This procedure was used in determining the varaition of the ratio of H to I described above, and it was only necessary to know the constants of such a set-up to enable one to make absolute determinations of the magnitude of the magnetizing field being examined. The constant, AN, the product of number of turns by average area of the turns, is one quantity whose value must be known very exactly. This constant was determined for the bobbin used by placing it inside a long solenoid which was very uniforly wound and all of whose physical quantities could be measured accurately, thereby making it possible to calculate the value of the magnetic field along its axis to a high degree of accuracy. The equation for this is

$$H=\frac{2\pi NI}{10L}\left[\frac{(D+L/2)}{((D+L/2)^2+R^2)^{1/2}}-\frac{(D-L/2)}{((D-L/2)^2+R^2)^{1/2}}\right]$$

where N = total number of turns in winding = 697
L = length of winding = 86.7cm
R = radius of solenoid = 3.81 cm
D = distance from center of solenoid in cm.

For such a solenoid, the variation of H from the mean value throughout a 7″ section at the center is approximately two hundredths of one per cent; the mean value is $H=10.06\ I$. Having obtained the deflection from the H-coil or bobbin when the current was reversed through the long solenoid, and the deflection from the secondary of the mutual inductance when the same value of current measured on the same ammeter was reversed through its primary, the required product is given by

$$AN=\frac{M\times 10^8}{10.06}\times\frac{D_H}{D_M}$$

where M = value of mutual inductance in henries
D_H = deflection from H-coil or bobbin
D_M = deflection from secondary of mutual inductance
AN = product of turns $\times$ area of the H-coil

A large number of such determinations was made using a wide range of currents, different mutual inductances, and different galvanometers. Naturally these determinations should be nearly the same, and the average of the whole series is believed to be very close to the actual value. The accepted value is

$$AN = 94,500 \text{ turns} \times \text{cm}^2$$

Likewise a great many tests were made to determine the ratio of H/I when the constant AN had been determined. Given the deflection from the H-coil due to a reversal of the magnetizing current in the permeameter and the deflection from the secondary of the mutual inductance due to a reversal of the current through the primary, this ratio is given by the equation

$$\frac{H}{I} = \frac{M \times 10^8}{AN} \times \frac{D_H}{D_M}$$

As stated above, this ratio was found to be sensibly constant. Slight variations were found in this value from one determination to another, but the average of a number of tests is believed to be very nearly the true value. The magnetizing force H, developed in the permeameter by a current of I amperes, was thus found to be given by the following relation.

$$H = 226I \text{ gil/cm}$$

As constructed, this permeameter has a fixed air-core bobbin or H-coil built in inside the magnetizing solenoid and so arranged that it is close and parallel to the bar being tested. This provides a means for determining H-values which is independent of the magnetizing current, if it is found desirable to do so. This coil is mounted in the uniform portion of the magnetizing field, as indicated in Fig. 3.

The second method of calibrating may be called an extrapolation method. The experiments just described show that a sensibly linear relationship exists between the magnetizing force and the magnetizing current. Several tungsten magnet steel bars were available which had been calibrated by the Bureau of Standards by the Class A test. We had made a number of tests on these bars and all data indicated that the values given by the Bureau of Standards were accurate to within

one or two per cent as their guarantee stated. Using these bars as standards, the J-permeamter was calibrated for coercive force determinations up to 55 gil/cm, the constant ratio of magnetizing force to magnetizing current permitting one to extend this calibration linearly up to coercive forces of 250 gil/cm. This method checks the absolute method very closely, and thereby gives strong supporting evidence that the calibration of the J-permeameter is correct.

OPERATION AND PERFORMANCE

A 110 volt D. C. supply is used when a magnetizing force of 1000 gil/cm is required as in the testing of cobalt magnet steel. For tungsten and chromium magnet steel, a 42 volt storage battery furnishes adequate current. A convenient testing circuit is shown in Fig. 6. This

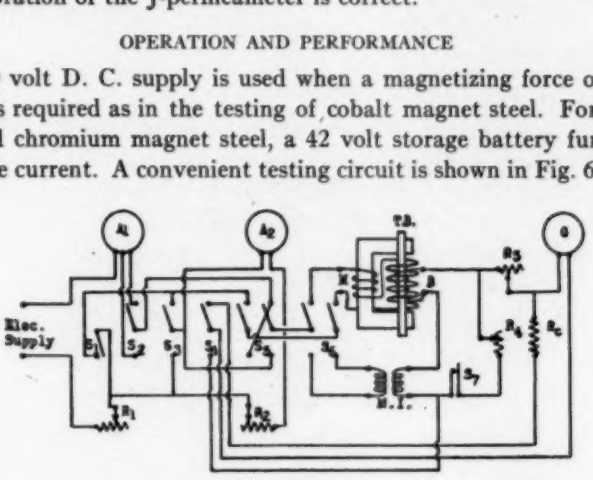

FIG. 6. *Showing a convenient system of electrical connections for the J-permeameter.*

A_1=Ammeter, 0-1 and 0-5 ampere ranges.
A_2=Ammeter, 0-1.5 ampere range.
B=B-Coil of permeameter.
G=Galvanometer or fluxmeter.
M=Magnetizing coil of permeameter.
$M.I.$=Mutual inductance.
R_1R_2=Rheostats.
R_3, R_4=Resistances.
R_c=Critical damping resistance.
S_1=Single-pole single-throw switch.
S_2, S_3, S_4=Single-pole, double-throw switches.
S_5, S_6=Double-pole double-throw switches.
S_7=Single contact key.
$T.B.$=Test bar.

circuit is essentially the same as that ordinarily used for ring tests; in fact ring samples with primary and secondary windings may be used interchangeably with the permeameter. The manipulation of the switches is precisely the same when using the permeameter as when testing ring samples, both as regards taking normal induction curves and in obtaining data for complete hysteresis loops. This is mentioned here because the demagnetization curves and hysteresis loops are of prime interest in studying magnet steels and in designing permanent magnets, and it is advantageous to be able to obtain such data easily and accurately.

In making the ordinary determination of saturation induction, residual induction, and coercive force, it is possible to test as many as 15 bars per hour, including proper calibrations, if their respective characteristics do not vary more than about 25% from one another. It is possible to repeat successive measurements to within 1% without difficulty. Measurements made at wide intervals of time can be duplicated to within 2 or 3% for coercive force, about half the variation allowed by the A. S. T. M. specification for testing magnet steel. Values of induction vary only by the errors incidental to calibration and observation, which amount to around 2% for ordinary testing, or 1% when sufficent care is exercised.

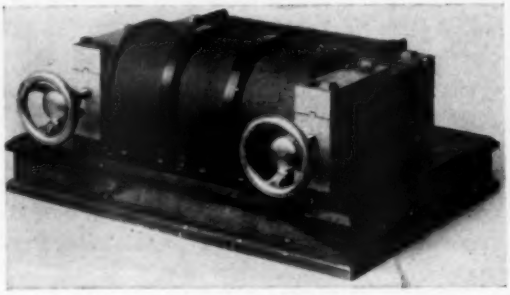

FIG. 6. *The assembled permeameter.*

CONCLUSIONS

From the foregoing discussion, it appears to be well established that the J-permeameter provides means for testing magnet steel with the following points that merit special attention.

1. A very uniform magnetizing force is developed throughout a wide range of values, including values sufficiently high for testing the best cobalt steel.

2. The magnetizing force is directly proportional to the magnetizing current. This makes its operation both simple and rapid, as values of magnetizing force are computed from ammeter readings.

3. An auxiliary coil is located in the uniform field adjacent to the bar being tested for the absolute determination of the magnetizing field if desired.

4. The *B*-coil is compensated for air flux, or in other words, ferric induction only is indicated. Such compensation is very desirable if not

essential for high accuracy when testing is done at magnetizing forces as high as 1000 gilberts per centimeter.

5. The accuracy of the instrument is all that can be expected, even of a precision instrument, for magnetic testing.

6. A test of magnet steel is reduced to the equivalent of a ring test, the simplest form of magnetic testing.

WESTERN ELECTRIC CO.,
HAWTHORNE STATION,
CHICAGO, ILLINOIS.

THE "ACID–ALKALIMETER"; A DIRECT-READING pH METER

By Kenneth H. Goode

The measurement of the acidity or alkalinity of solutions has become increasingly important in chemical investigation, and in the control of chemical processes in industry The acidity or alkalinity of a solution depends upon the concentration of the hydrogen ions present in it, and is numerically expressed as the "pH" value of the solution, which is defined as the negative logarithm of the hydrogen ion concentration. Thus the pH of a solution usually lies somewhere between 0 (strong acid) and 14 (strong alkali); the point of neutrality, corresponding to the pH of pure water, being 7.

The pH of a solution may be determined by the use of a suitable indicator or combination of indicators, or by measuring the electrical potential between suitable electrodes, one of which has been placed in the solution. Although indicators provide a convenient, and in some cases an accurate means of determining pH, the electrical method possesses several advantages. These advantages make possible the design of an instrument which will indicate the pH directly upon a scale, and can be made to record this value automatically, and if necessary to maintain the pH of a vat or system at any desired value, by means of suitable relays and valves. Such an instrument will be described in this article.

In determining the pH of solutions by the electrometric method two electrodes are necessary. One of these, the indicating electrode, is placed in the solution whose pH is to be determined, and its potential relative to the solution is a function of the pH of the solution. The other, the reference electrode, is placed in a solution of such a nature that its potential relative to this solution is constant. The two solutions are connected by a "salt bridge." The potential between the two electrodes is then a function of the pH of the solution. The hydrogen electrode is the most important of the indicating electrodes, and the calomel half-cell the most convenient of the reference electrodes. If this combination of electrodes is employed, the potential between them is given by the equation:

$$E\,(\text{volts}) = 0.25 + 0.058(\text{pH})$$

Thus the potentials encountered will lie between 0.25 and 1.06 volts. However this relation only holds good when no current is being drawn from the electrodes. For this reason an ordinary voltmeter cannot be used, and we must either use a potentiometer or an electrostatic voltmeter. Goode[1] in 1921 showed that a three-element vacuum tube could satisfactorily be employed in measuring pH, and designed an apparatus for this purpose. The circuit was that of Fig. 1, the potential to be measured being applied to the grid of the vacuum tube. That part of the plate current which was proportional to the pH was measured by a galvanometer, which could be calibrated directly in pH units.

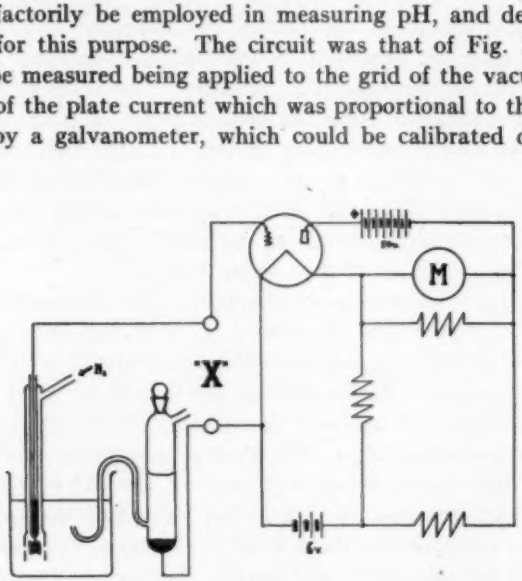

FIG. 1. *Circuit of original instrument.*

An instrument of this type has certain disadvantages which hinder its application in the laboratory. Because of the small currents which are measured, it is necessary to use either a galvanometer or a micro-ammeter. The former is inconvenient, and the latter is expensive and delicate. Further, the calibration of such an instrument is affected by a number of factors, all of which must be kept constant if it is to remain correct. Among the most important of these factors are the *B* battery voltage, the *A* battery current, and the condition or efficiency of the vacuum tube used. Bienfait[2] has described an ingenious modification of the circuit, in which the effect of change

[1] Goode, "A Continuous Reading Electrotitration Apparatus," J. Am. Chem. Soc., *44*, p. 26; 1922.

[2] Bienfait, "A Deflection Potentiometer," Receuil des Travaux Chimiques des Pays-Bas, *46*, p. 166; 1926.

in *B* battery voltage is compensated. He found it necessary to place the apparatus in an oil bath to insure a constant *A* battery current. Recently Pope and Gowlett[3] have found it possible to dispense with the *B* battery entirely, by making use of a 4–element vacuum tube, and the *A* battery current is adjusted to a fixed value before and after each reading.

In the original apparatus described by Goode, a vacuum tube having a pure tungsten filament was used. This type of tube was found to be very sensitive to slight changes in temperature and to filament current fluctuations. In both Bienfait's and Pope and Gowlett's instruments, as well as in later instruments described by Goode, thoriated filament tubes were used. This represents a great improvement over pure tungsten, but the writer has found it practically impossible to use a thoriated filament tube over periods of many hours without having the electron emission, and therefore the characteristics of the tube, change noticeably. Filaments of the oxide-coated type are practically free from this trouble, and therefore are strongly recommended. Oxide coated filament tubes have been used continuously over periods of several days without noticeable change in their electron emission. This is particularly the case when the filaments are burned somewhat below their rated temperature.

The chief objection to the use of a single vacuum tube in designing a pH meter is the necessity of using a microammeter or millivoltmeter as the indicating device. A marked decrease in cost and increase in ruggedness and portability is possible if a milliammeter is used instead, and this is possible if additional vaccum tube amplification is used. A hydrogen ion meter using three tubes has been described by Goode[4]; the simplified circuit being shown in Fig. 2. The indicating device in this instrument is a milliammeter (0-3 milliamps.), which can be calibrated directly in pH units. The same meter is used as a voltmeter for calibration purposes, and also in adjusting the filament current to a definite value. This necessitates a somewhat complicated switching arrangement. Bienfait has justly criticized this apparatus as being too complicated, and after using this instrument over a period of more than a year, the writer has found it rather difficult to adjust and to keep in adjustment. The principal difficulty

[3] Pope and Gowlett, "A Direct Reading Hydrogen Ion Meter," J. Sci. Instruments, *4*, p. 380; 1927.

[4] Goode, "An Improved Continuous Reading Hydrogen Ion Meter," Journal Am. Chem. Soc., *47*, p. 2483; 1925.

however was found to be changes in the characteristics of the tubes used, rather than changes in the battery voltages. For this reason thoriated filament tubes have been abandoned by the writer in favor of the oxide coated type, and in changing to the latter type of tube it has been found possible to use only two tubes instead of three, with a consequent simplification of the circuit.

Thus there have been developed two new types of pH indicating meter; which are easy to adjust, remain in adjustment over long periods of time, are readily portable, and have been found to be satisfactory under the rigorous conditions of actual use in the laboratory by untrained persons.

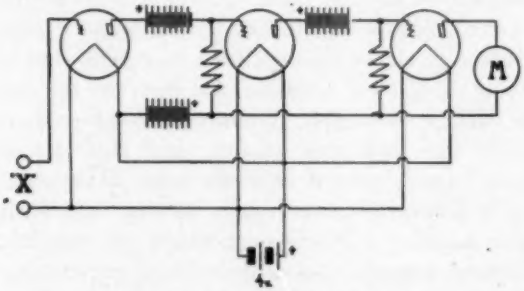

FIG. 2. *Circuit of three-tube instrument.*

Only a few varieties of oxide coated filament tubes are available in the United States at the present time. Of these, two types manufactured by the Western Electric Co. were found to have particularly suitable characteristics. One of these, the "101-D" tube is capable of handling several times as much plate current as the tubes previously used. This means that there need be no saturation with its consequent distortion of the pH scale. The other, the "102-D" tube, has a high amplification constant, which makes it possible to secure enough amplification although using only two tubes instead of three. The elimination of one tube also means the elimination of the third "B" battery, and a great simplification of the circuit.

The filament characteristics of these tubes differ from those of the tubes previously used. The 101-D operates with a filament voltage of 4 volts, while the 102-D requires only 2 volts. The filament current however being the same (0.95 amperes) in each case, the tubes can be placed in series instead of in parallel, and thus operated from one six volt storage battery. It is found that satisfactory results are

obtained with filament currents as low as 0.80 amperes, and the constancy of the electron emission as well as the life of the tubes is greatly improved at this value. In order that the filament current may be kept constant, an ammeter having a one ampere range is kept permanently in the filament circuit. This use of a separate ammeter simplifies the final circuit considerably.

The indicating device is a special Weston three terminal voltmeter-milliammeter. The scale is calibrated in volts from zero to 1.5, and directly in pH units from zero to 14; each unit of pH corresponding to 0.2 milliamperes. A Model 269 meter is used, which is somewhat larger than the Model 280 previously used, and much easier to read. The readings are accurate to 1 per cent, which corresponds to 0.15 pH.

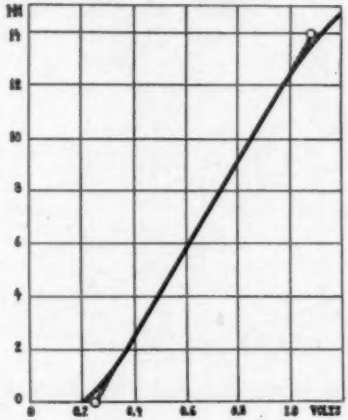

FIG. 3. *Calibration curve of acid-alkalimeter.*

In order to adjust the instrument so that the pH calibration of the meter is correct, it is necessary to adjust the various resistances in the circuit to their proper values. In Fig. 3 the reading of the milliammeter, pH, is plotted against the value of the potential measured. The correct calibration curve is a straight line between the points indicated by the circles. The calibration curve actually obtained resembles more often the curve shown. The deviations at the top and bottom can be largely elimineted, and will be discussed later.

The circuit is shown in simplified form in Fig. 4. Four controls: *A*, *B*, *C*, and *Q*, are provided to adjust the instrument to the correct calibration curve. Rheostat *B* is adjusted so that the filament current

is 0.80 amperes. The value of A determines the slope of the straight portion of the calibration curve. C and Q serve to shift the calibration curve to the right or left, although they have other functions which will be discussed later. In order to get a correct calibration curve it is only necessary to adjust A, C, and Q to the correct values. Adjustment of the B battery voltages is not necessary, and in fact changes in the values of these voltages can be compensated by adjustment of A, C, and Q.

In order to understand the effect of the controls C and Q, it is necessary to refer to Fig. 5, which shows the plate current and the grid current of a 102-D vacuum tube, plotted against the potential applied to the grid. It will be seen that grid current flows whenever

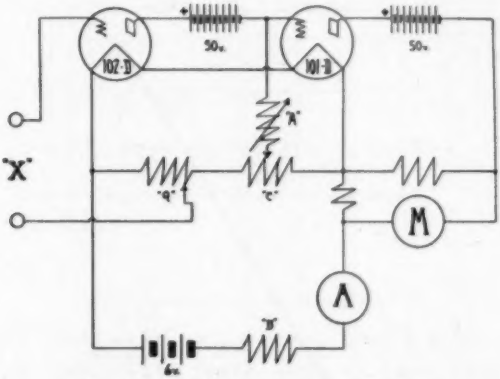

FIG. 4. *Simplified circuit of acid-alkalimeter.*

the potential of the grid becomes more positive than 0.75 volt; the potential being referred to the positive end of the filament. We cannot therefore connect the potential to be measured simply between the positive end of the filament and the grid, because current would be drawn from the electrodes whenever the pH became less than 8.6. On the other hand, we cannot connect it simply between the grid and the negative end of the filament (about -1.5 volt) because the plate currents would then not change linearly with the grid potential, and the result would be a distortion of the pH scale. Thus the function of the potentiometer Q is to add to the unknown potential a sufficient amount so that no grid current flows at any pH, and yet operate the tube on the straight portion of the plate current curve. In the case shown, an added Q potential of 0.60 volts would be an optimum ad-

justment, since the potentials encountered between pH=0 and pH=14 would range between 0.85 and 1.66 volts.

A curve similar to Fig. 5 might be drawn to represent the plate and grid currents in the 101-D tube. In this case the curved portion of the plate current curve is avoided by arranging a circuit to balance out the first 1 or 2 milliamperes of the plate current. This eliminates almost entirely the tendency to deviate at the bottom of the calibration curve of Fig. 3.

It should be noted that the plate current of the 102-D tube, as shown in Fig. 5, is not what is measured by the milliammeter, but causes a change in the grid potential of the 101-D Tube which in turn controls the current through the milliammeter. For this reason curvature of the plate current curve at the lower end causes a deviation downward at

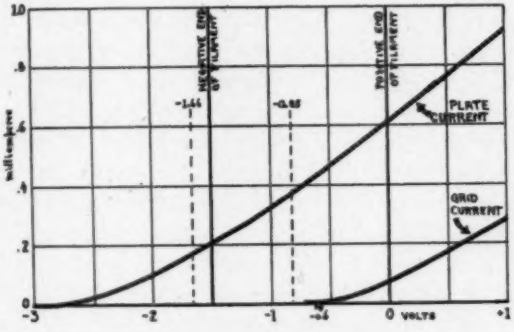

FIG. 5. *Illustrating effect of plate and grid currents.*

the upper end of the calibration curve. This is the cause of the deviation at the upper end of the curve of Fig. 3. It can be minimized by using no more Q potential than necessary to prevent current drain from the electrodes. A fixed value of Q potential might be used, were it not for the fact that 102-D tubes are not at all uniform in this respect. The value of 0.75 volt given above is to be considered as the value for a particular tube; another tube might require as much as half a volt more or less than this much. The correct value is easily ascertained by leaving the grid unconnected, and noting the meter reading. Since no current is flowing, the grid automatically assumes the potential in question, except when affected by stray currents or electrostatic charges.

Potentiometer *C* is then adjusted so that the milliammeter reads somewhat less than zero, and a potential of 0.25 volts is applied to the grid, and *Q* adjusted until the milliammeter reads zero. This gives a rough idea of the adjustment of *C* and *Q*, and they are then further adjusted, together with *A*, until the pH reading for 0.4 volt is 2.6, and for 1.0 volt is 12.9 (two points on the theoretical calibration curve). When this has been done, the pH readings can be depended upon, except for possible slight errors at the extreme ends of the scale.

In order to make it possible to calibrate the instrument at any time, and to provide a standard potential with which to compare the unknown potential, the potentiometer *K* is provided. By means of the switch *S* either this known potential or the unknown potential is applied to the grid of the 102-D tube. The complete circuit is shown in Fig. 6. When the switch *S* is down, the unknown potential is applied to the grid, the meter (when correctly adjusted) reading pH. When the switch is in the center position, the potential *K* is applied to the grid, and the meter reads the pH (when correctly adjusted) corresponding to this potential. When the switch is up, the meter reads the potential of *K* directly in volts. By adjusting *K* until the meter reads the same, whether down or center, the unknown potential may be determined by throwing the switch up.

Since the same meter is being used as a voltmeter and as a milliammeter, it is necessary to replace the voltmeter by a resistance of 500 ohms when the milliammeter is being used. This is also done by means of the switch *S*.

The possibility of grid current flowing in the 101-D tube does not cause trouble, because under ordinary conditions of adjustment the grid of this tube is too negative, and even if a slight grid current should flow, its effect tends to compensate for the deviation at the upper end due to the 102-D tube.

The two *B* batteries used may be of any voltage from 45 to 150 volts; the higher voltages giving straighter calibration curves. Values of 67.5 volts each are satisfactory. A 6-volt lead storage battery, having as large a capacity as convenient, is used to light the filaments. Edison storage batteries are not recommended, as their voltage changes with use, which makes necessary frequent readjustment of the filament current.

The variable resistance *A* is a most important part of the circuit, as its value must not change after being once adjusted to a correct

value. (The only type which has been found to be entirely satisfactory is a 50,000 ohm wire-wound unit made by the Central Radio Laboratories, of Milwaukee.)

Besides its use in calibrating the instrument to read pH, the adjustment Q has a function which is of importance when other electrodes than the hydrogen electrode are used, such as the quinhydrone, antimony, and tungsten electrodes. These electrodes follow laws

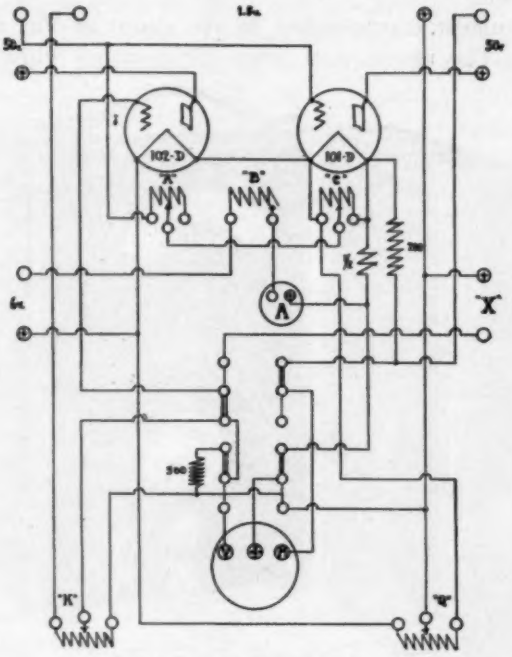

FIG. 6. *Complete circuit of D.C. model.*

similar to that of the hydrogen electrode, except that the constant term is different. Thus the quinhydrone electrode follows the equation:

$$E\,(\text{volts}) = -0.45 + 0.058(\text{pH})$$

Thus readings made with the quinhydrone electrode and calomel cell are all 0.70 volts less than they would be if made with the hydrogen electrode. To use the quinhydrone electrode, the instrument is first adjusted to read pH according to the hydrogen electrode. The X

terminals are then short-circuited (first removing the electrodes) and Q adjusted so that the meter reads 7.8 pH units. The instrument will then read pH correctly for the quinhydrone electrode, the short-circuit having been removed, and the electrodes reconnected to the X terminals. Other electrodes can be used in a similar way, although there is more doubt as to the validity of the corresponding equations. For the antimony and tungsten electrode the difference appears to be about 0.3 volt.

The instrument, corresponding to the circuit of Fig. 6, is shown in Fig. 7. The two vacuum tubes are mounted within the case,

FIG. 7. *D.C. model of acid-alkalimeter.*

upon a sub-panel directly behind the ammeter, where they are protected from stray electrostatic charges, as well as from breakage. The batteries and electrodes are connected to binding posts on the front panel.

If a record of the pH is desired, a recording meter may be connected in series with the milliammeter. The operation of the instrument is exactly the same as before, except that a slight readjustment

may be necessary. The recording meter should be one having a maximum deflection corresponding to 3 milliamperes; while the chart used should be graduated from zero to 15, to read pH units directly.

Tests of the operation of the instrument together with a recording meter over long periods show a gradual drift for the first 5 or 6 hours, corresponding to a decrease of about 0.5 unit of pH, after which the reading is steady within less than 0.1 pH until the filament battery is discharged. This drift is due to a slight decrease in voltage in the *B* batteries.

Since there is some demand for an instrument that may be used for continuous indication of pH over long periods of time, another form of acid-alkalimeter has been developed which operates directly from the 110 volt A.C. lighting circuit. In this instrument the filaments of the vacuum tubes are lighted by means of a special transformer having one 2 volt and one 4 volt secondary. The plate potentials are supplied by a transformer together with a UX–280 full-wave rectifier tube, which supplies a current of 40 milliamperes at 150 volts. A filter circuit to provide pure D.C. is advisable, but can dispensed with if necessary. All batteries are eliminated except the one dry cell which supplies the *K* potential.

The circuit used in this case is slightly different from that of the battery operated instrument, and is shown in Fig. 8. The method of adjustment is the same, except that *C* has been dispensed with. To make the meter read pH units directly, *A*, *Q*, and *K* are adjusted exactly as before.

This arragnement is subject to one drawback; the calibration of the meter is sensitive to slight changes in the "110 volt" line voltage. For example, when the line voltage changes from 105 to 85 volts, the pH reading changes from 10.0 to 12.2. To obtain a steady reading within 0.1 pH unit, it is necessary to have a line voltage steady within one volt. This requirement is fulfilled in some localities, but in many others the line voltage is not this steady.

In order to make the readings more independent of line voltage fluctuations, an iron wire ballast lamp (manufactured by the General Electric Co.) is placed in the primary circuit of the transformer, the primary windings being designed for 50 volts instead of 110 volts. With this ballast lamp in the circuit, the pH reading changes from 10.0 to only 10.5 when the line voltage changes from 105 to 85 volts, and the permissible fluctuation of the line voltage becomes 5 volts instead of 1. A voltmeter is placed across the primary windings, and the fila-

ment current is controlled by changing the resistance *B*, which is adjusted until the reading is 45 volts. Because of the characteristics of the ballast tube, the current drawn from the line is about one ampere, corresponding to about 100 watts of power, most of which is dissipated as heat in the ballast tube and the resistance *B*.

This A. C. operated instrument may be assembled as a single unit, requiring only to be plugged in to the lighting socket, and connected to the electrodes; or it may be assembled as two separate units, connected by a 4-wire cable. The dotted line in Fig. 8 indicates where

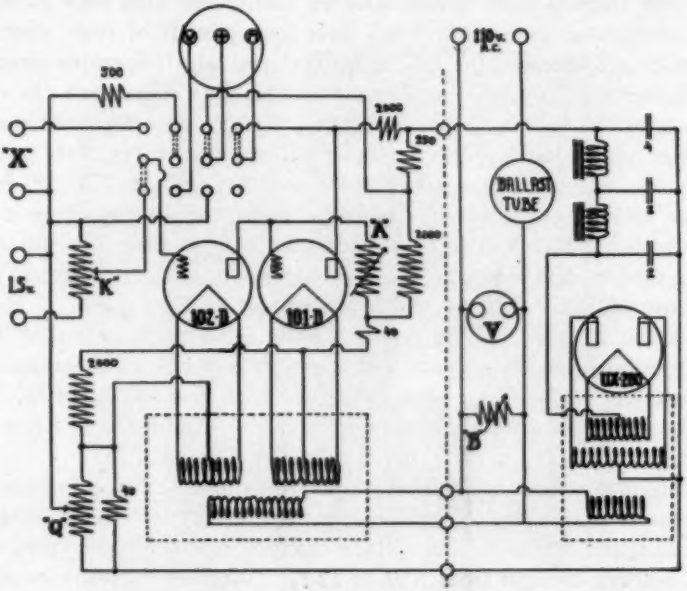

FIG. 8. *Complete circuit of A.C. model.*

the separation may be made, if desired. The *B* control and voltmeter may be placed in either unit.

The two types of acid-alkalimeter which have been described were designed specifically to include the whole pH scale from zero to 14, and as a consequence the accuracy with which a pH reading may be made is of the order of 0.1 pH unit. This is amply sufficient accuracy for ordinary laboratory and industrial purposes, because of the inaccuracies in the electrodes used. Electrodes which act as they should are exceptional, and even if a perfect electrode were used, a change in temperature of

2°C might make an error as great as 0.1 pH unit. However, under the more strictly regulated conditions of biochemical research, a higher degree of accuracy is required. It is therefore of interest to consider how accurate an instrument of this type might be made.

A milliammeter having a maximum range of 1.5 milliamperes is available; if this were used, and if A were made to have near 100,000 ohms, it is possible to have the full-scale reading correspond to 4.0 pH units or 0.24 volts. The accuracy of the pH reading would be about 0.04 pH units. In this case the pH reading would be relative rather than absolute. Thus, after calibration, one point of the scale would have to be set at a known pH before any readings would have any significance. This could be easily done, for example, by placing the electrodes in a buffer solution of known pH, and adjusting Q until the meter reads some convenient arbitrary value. Any pH reading subsequently made would be referred to this as a standard. Thus if a buffer having a pH of 7.00 were used, and the meter set at the center of the scale, the range of pH would be from 5.00 to 9.00.

The development of the two types of acid-alkalimeter which have been described in the article has been carried out with the cooperation of the Division of Industrial Research of the Pennsylvania State College.

DEPARTMENT OF CHEMISTRY,
STATE COLLEGE, PENNSYLVANIA.

THE MEASUREMENT OF HIGH D. C. POTENTIAL DIFFERENCES WITH APPLICATIONS TO THE CALIBRATION OF ELECTROSCOPES AND ELECTROSTATIC VOLTMETERS

By Wm. Bender

ABSTRACT

An arrangement of condensers, switches, and a ballistic galvanometer is discussed, by means of which high D.C. potential difference can be measured with considerably greater precision than given by ordinary high voltage electrostatic voltmeters. Simple equations of design are derived, which if scrupulously followed will give 0.5% (and greater) accuracy no matter how high the D.C. potential difference. The application of this method to the calibration of an electroscope is given in detail.

In the measurement of d. c. voltages (say 600 volts and upwards, i.e. just outside of the ordinary electromagnetic voltmeters ranges) where greater precision is required than available in the usual electrostatic voltmeters, the following arrangement may be used to advantage.

The P. D. to be measured is applied to a number of condensers in series, as shown in Fig. 1. The theory of the arrangement follows:

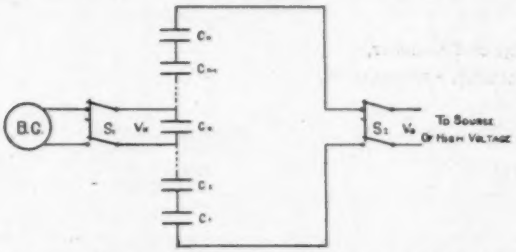

Fig. 1. *Circuit diagrahm for measuring high dc potential differences.*

Let V_0 = the potential difference to be measured.

Let $V_1, V_2, \cdots V_n$ = the potential differences across the several capacitances $C_1, C_2 \cdots C_n$ when S_2 is closed. Then,

$$V_0 = V_1 + V_2 + \cdots + V_k + \cdots + V_{n-1} + V_n$$

$$= Q\left(\frac{1}{C_1} + \frac{1}{C_1} + \cdots + \frac{1}{C_k} + \cdots + \frac{1}{C_{n-1}} + \frac{1}{C_n}\right) \qquad (1)$$

If G is the ballistic constant of the galvanometer, and d is the deflection produced by Q, the charge in each condenser, we have,

$$V_0 = Gd\left(\frac{1}{C_1}+\frac{1}{C_2}+\cdots+\frac{1}{C_k}+\cdots+\frac{1}{C_{n-1}}+\frac{1}{C_n}\right) \tag{2}$$

$$\text{If } C_1=C_2=\cdots=C_k=\cdots=C_{n-1}=C_n=C \tag{3}$$

$$\text{then (2) becomes, } V_0=\frac{Gn}{C}d \tag{4}$$

It is to be noted here under these conditions, also, that,

$$V_1=V_2=\cdots V_k=\cdots V_{n-1}=V_n=V \tag{5}$$

The choice of the number of condensers to be used and the capacitance of each in measuring a given potential difference with a given galvanometer is governed by three factors:

1. The quality of the insulation of the ballistic galvanometer coil.
2. The maximum safe operating voltage of the condensers used.
3. The ballistic constant of the galvanometer.

1. Let N = the number of turns of the ballistic galvanometer coil. The voltage between turns will be V/N initially, or

$$\frac{V_0}{N}\frac{1}{n}.$$

This must be small enough so that the galvanometer will not be injured. If V_b' is the insulation break down voltage between galvanometer coil turns, then, for satisfactory performance,

$$\frac{V_0}{N}\frac{1}{n}<V_b' \text{ or } n>\frac{V_0}{NV_b'} \tag{6}$$

2. V must be less than any value which will injure the dielectric or change the rated capacity of the condensers used, i.e., if V_b'' is the maximum safe voltage across any condenser, (the potential difference above which the condenser will change its rated value, temporarily or permanently), $V_0/n\ (=V)<V_b''$ or

$$n>\frac{V_0}{V_b''}, \tag{7}$$

for satisfactory performance.

3. For a given ballistic galvanometer and a given applied potential difference,

$$V=\frac{V_0}{n}$$

But

$$Q=CV=C\frac{V_0}{n}=Gd$$

Hence

$$\frac{C}{n}=\frac{Gd}{V_0} \tag{8}$$

Choosing a value of d well out on the scale C/n can be approximately determined.

Summarizing, then, we have,

$$n>\frac{V_0}{NV_b'} \tag{6}$$

$$n>\frac{V_0}{V_b''} \tag{7}$$

$$\frac{C}{n}=\frac{Gd}{V_0} \tag{8}$$

Having determined a value for n from (6) and (7) the value of C may be had from (8). We must note that (6) and (7) must be satisfied simultaneously.

When conditions (3) and (5) can not be realized equations corresponding to (6), (7) and (8) can readily be derived if we know the capacity of each condenser to be used and the approximate potential difference to be measured. Thus, for example, $Q=C_kV_k$

$$C_k=\frac{Gd}{V_k}=\frac{Gd}{V_0-Gd\left(\frac{1}{C_1}+\frac{1}{C_2}+\cdots+\frac{1}{C_{k-1}}+\frac{1}{C_{k-1}}+\cdots+\frac{1}{C_k}\right)}$$

which corresponds to (8), etc.

If we assume in (5) and (6) a safety factory of 50% we may write

$$n=1.5\frac{V_0}{NV_b'} \tag{5'}$$

and

$$n=1.5\frac{V_0}{V_b''} \tag{6'}$$

which may be used as equation of design. The larger value of n is to be used in (8).

CALIBRATION OF AN ELECTROSCOPE

The circuit diagram used to calibrate an electroscope is shown in Fig. 2. The high voltage source was a rectifier giving approximately 1500 volts D. C. With switch S_1 closed and S_2 open, the leaf of the electroscope, E, stood out at right angles. By opening S_1 and closing S_2 the leaf of the electroscope could be brought to any desired point on its scale, the P. D. between its terminals being lowered by leakage of charge through the very high leak resistance R. Then S_3 is opened and S_2 is closed. The voltage across the electroscope is then given by (2), in which V_0 is to be taken as the voltage across the electroscope just before closing switch S_3. As the voltage drop across the electroscope is decreased by means of further leak, it may be necessary to increase C_k by adding more capacitance to it in shunt. Formula (2) will again give the voltage at its terminals. Thus the electroscope can be calibrated throughout its entire range.

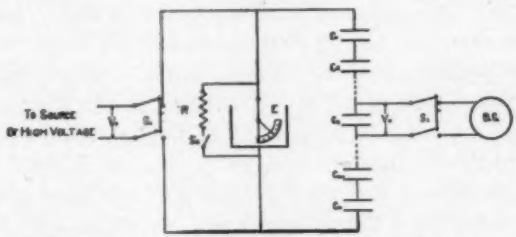

FIG. 2. *Circuit diagram for the calibration of an electroscope.*

This method may be used to calibrate other types of electrostatic voltmeters with considerable precision if the precautions given in (6) and (7) are observed, and is particularly valuable where a variable source of high D. C. voltage is not available.

Some idea as to the precision of calibration of high voltages may be had by a consideration of the following facts:

In the equation,

$$V_0 = Gd\left(\frac{1}{C_1}+\frac{1}{C_2}+\cdots+\frac{1}{C_k}+\cdots+\frac{1}{C_{n-1}}+\frac{1}{C_n}\right)$$

G may be measured with an accuracy of 0.5%; d with a consistently reproducible accuracy of 0.5% in a well constructed galvanometer, and the C's with an accurracy of 0.25% this last percentage being guaranteed by reliable firms manufacturing condensers. Thus an

accuracy of 1% is easily realizable and with many condensers, the errors in C tend to cancel, so that 0.5% error and less is realizable in the final measurement provided only the precautions in (6) and (7) are adhered to.

Having calibrated an electrostatic voltmeter, the voltmeter in conjunction with the condenser-divider can be used in A. C. and D. C. circuits as a multiplier, as is well known. If the arrangement is used as a multiplier in an A. C. circuit, and if V_0 is the root-mean-square value of the voltage to be measured, the safety factor, 50%, will guard against dielectric breakdown due to the peak value of the A. C. voltage.

PHYSICS DEPARTMENT,
LEHIGH UNIVERSITY.
BETHLEHEM, PA.

A RADON PUMP*

By L. F. Curtiss

This paper describes a pumping system for removing radon from a solution of radium salts. Several improvements have been made which make it more efficient and easier to manipulate than the usual forms. The chief advantages of this design are that it eliminates all rubber tubing and all stopcocks through which mercury must pass. This avoids the annoyances from dirty mercury which are otherwise encountered. The arrangement here described makes the use of liquid air very convenient and therefore permits somewhat more rapid manipulation than is possible with a pump depending solely on purification by chemical means. The only stopcock in the whole apparatus is between the drying bulb and the radium bulb. Although this is exposed to the radon it has given no trouble during the year which this outfit has been in use in the radium laboratory at the Bureau of Standards. All gaseous products which develop from the grease used on this stopcock are apparently removed by the subsequent purification.

Fig. 1 is a scale drawing of the pump. The radium bulb, stopcock and sparking bulb are not shown but would be attached to the open tube leading from the P_2O_5 bulb in the upper part of the figure. The apparatus consists of two Toepler pumps in series with a few accessories to provide for purification of the radon and for manipulating the mercury in the pumps. In operation the impure radon is drawn from the bulb containing the radium solution through a small sparking bulb provided with electrodes between which the spark from a small induction coil continually passes. This ignites the hydrogen and oxygen. The moist mixture then passes over through the P_2O_5 bulb where all water vapor is removed if sufficient care is taken. The gases then pass over molten KOH to remove CO and CO_2 and finally over heated copper oxide to remove any excess of hydrogen. The radon as finally drawn into the bulb of pump No. 1 is comparatively pure but may contain small amounts of permanent gases. These are removed by pumping the radon over into the vertical tube supporting the Dewar, *D*, which has been previously evacuated by pump No. 2. As soon as all

* Publication approved by the Director of the Bureau of Standards of the U. S. Department of Commerce.

the gas containing the radon has been pumped over, the mercury level being held above the side arm going to pump No. 2, liquid air is poured into the Dewar and after ten or fifteen minutes the residual uncondensed gases are pumped off by pump No. 2. Then the liquid

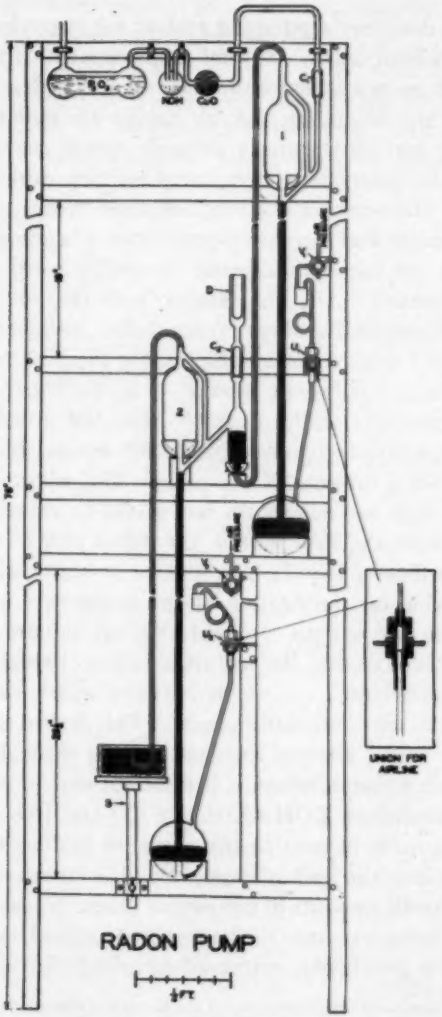

FIG. 1. *Assembled radon pump.*

air is removed and after a few minutes the radon in a fairly pure state may be pumped off and collected over mercury from the delivery tube of pump No. 2. If a higher degree of concentration is required it may be allowed to stand for several hours in contact with KOH.

The above method is suited for preparing radon for an exposing apparatus where it is desired to make sources of the active deposit RaB+C. However the design may be modified slightly so that it may be used either for this purpose or for filling small glass tubes with radon itself. The only modification required is in the Dewar. The

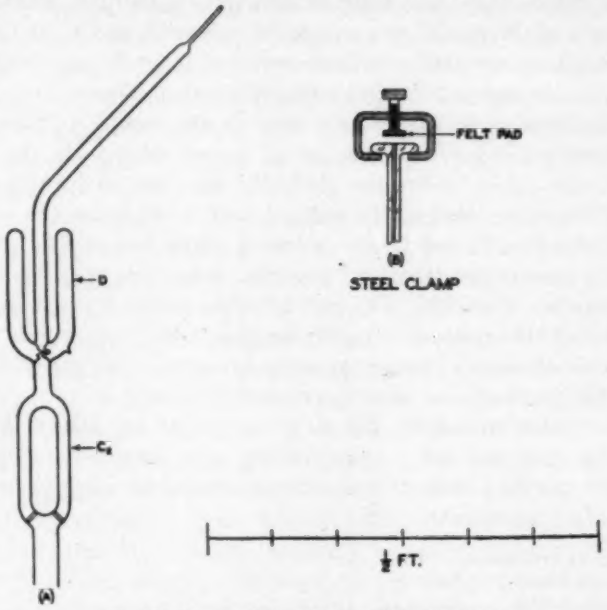

FIG. 2. *Dewar and clamp for use with radon pump.*

Dewar in Fig. 1 must be replaced by one as shown in Fig. 2*A*. The general operation remains the same but instead of pumping the radon off after removing the liquid air it is forced up through the central tube of the Dewar into the capillary where it may be sealed into the glass tube. When forcing the mercury up for this purpose it is necesary to prevent an excessive loss of mercury through the delivery tube of pump No. 2. The small clamp shown in Fig. 2*B* fits over the end of the delivery tube and effectually prevents the escape of mercury during this operation.

A few other details of the pumping system should be described. C_1 and C_2 are glass check valves ground into their upper seat to prevent mercury from rising above them. When the arrangement shown in Fig. 2*A* is used it is desirable still to include the check valve. Unless very carefully ground it will leak mercury fast enough to provide for forcing the radon into the capillary and it prevents a rapid rush of mercury into the stem of the Dewar when filled with liquid air which of course will break the Dewar. The mercury reservoirs for the two pumps are connected each to their respective pump by a barometric column and the top of each reservior has a small glass tube sealed into it. By means of the special two-way metal valves V_1 and V_2 these reservoirs may be connected to an air reservoir of about 25 pounds pressure or to the atmosphere. Thus by proper manipulation of these valves the mercury may be run up and down in the pumps without lifting any reserviors and without the use of rubber tubing. In the course of operation these reservoirs gradually lose mercury which passes over through the pumps. To make it easy to replenish the mercury two steel unions U_1 and U_2 are provided. Since four or five "strokes" suffice to remove practically all available radon this does not require very frequent attention. The part attached to the glass tubing running down to the reservoir is rigidly supported on the angle-iron framework while the upper part of the union attached to copper tubing can be readily taken off and allow mercury to be poured in.

If the bulbs containing the KOH and CuO are about the sizes indicated they will not require refilling over long periods of time. However the P_2O_5 bulb under ordinary conditions must be renewed about every six months.

BUREAU OF STANDARDS,
WASHINGTON, D. C.
APRIL 5, 1928.

AN EXHIBIT OF OPTICAL INSTRUMENTS AND OPTICAL PRODUCTS BY THE OPTICAL SOCIETY OF AMERICA

Under the joint auspices of the Optical Society of America and the Bureau of Standards there will be an Exhibit of Optical Instruments and Optical Products in the buildings of the Bureau at Washington, D. C. This exhibition will be open from 9:00 to 4:30, October 31, November 1, 2 and 3 and for one evening session to be designated later by the Optical Society. It is considered particularly appropriate that such an exhibit be held at Washington as, in addition to the visiting members of the Optical Society, there is the large group of scientific workers of the Government and institutional scientific establishments who are extensive users of optical instruments in their work and by whom novel applications of optical principles are being developed and applied.

It is the desire of the Committee to include in this exhibit all the newer instruments which have been developed by scientific investigators and our commercial firms. Research workers are particularly invited to contribute exhibits designed to illustrate the progress of their work and their attention is called to the fact that such an exhibit is often more useful than the presentation of a formal paper for emphasizing the significance and importance of an investigation. All American made instruments or products in which the application of optical principles is an important part in design, construction or use are eligible for exhibition. The following list will serve to partially indicate the contemplated scope of the exhibit: optical and colored glasses, fused silica, optical components, spectacle lenses, ophthalmic instruments, binoculars, microscopes, photographic apparatus, colored photographic processes, motion picture apparatus, astronomical instruments, interferometers, spectral apparatus, metrological instruments, surveying and nautical instruments, search lights, telescopic gunsights, photometric apparatus, optical pyrometers, colorimetric instruments, vacuum discharge tubes, special systems of illumination etc.

Those having appropriate material which they desire to exhibit are cordially invited to correspond with the undersigned chairman for further details relative thereto.

BUREAU OF STANDARDS,
WASHINGTON, D. C.

I. C. GARDNER, Chairman,
Committee on Optical Instruments Exhibit

Prize Offered by Scientific Apparatus Makers of America.—At the annual meeting in Atlantic City, May 4, 1928, the Scientific Apparatus Makers of America voted unanimously to offer a prize of two hundred and fifty dollars for the best paper on a non-optical instrument published in the Journal of the Optical Society of America and Review of Scientific Instruments during the year 1929.

A similar prize for the year 1928 was offered at the preceding annual meeting, full details concerning which appear in the advertising columns. The prize offered for the year 1927 will be awarded at an early date by a committee consisting of Professor C. E. Mendenhall, Professor A. G. Worthing, and Dr. L. O. Grondahl.

The Journal and its readers express their appreciation for the interest of the Apparatus Makers in stimulating research in Instrument Design and desire to thank the board of award for its careful consideration, still in progress, of the large number of papers eligible for the 1927 prize. (May 23, 1928.)

California Optometrists Association.—Two cities were hosts to the twenty-second annual convention of the California Optometrists Association this year. On June 4 the convention met in San Francisco and after two days adjourned to Los Angeles for two days further session. Over 250 delegates attended and the convention was one of unusual interest. The class in eye dissection was under Dr. Elmer Jones, of the Los Angeles School of Optometry, while the following well known leaders were among those listened to by the convention: Professor Frank Weymouth and Dr. Walter Milies of the Leland Stanford University; Scott Sterling, of the scientfic, staff of the Bausch and Lomb Company; and Dr. Karl Waugh, of the University of Southern California. Meetings were held at the famous old Hotel Alexandria. Next year's place of meeting has not been selected as yet.